

**A NOVEL CONSTANT FORCE COMPLIANT GRIPPER
DESIGN**

**SABİT KUVVET ÜRETEN ÖZGÜN BİR ESNEK TUTUCU
TASARIMI**

MEHMET OĞUZ ÖZTÜRK

PROF. DR VOLKAN PARLAKTAŞ

Supervisor

PROF. DR. ENGİN TANIK

Co-Supervisor

Submitted to

Graduate School of Science and Engineering of Hacettepe University

as a Partial Fulfillment to the Requirement

for the Award of the Degree of Master of Science

in Mechanical Engineering

April 2023

ABSTRACT

A NOVEL CONSTANT FORCE COMPLIANT GRIPPER MECHANISM DESIGN

Mehmet Oğuz ÖZTÜRK

Master of Science, Department of Mechanical Engineering

Supervisor: Prof. Dr. Volkan PARLAKTAŞ

Co- Supervisor: Prof. Dr. Engin TANIK

April 2023, 64 pages

The aim of this thesis is to design a novel constant-force compliant gripper mechanism. The design is a monolithic holding mechanism which is fixed on one side and free on the gripper side. The mechanism has four compliant hinges and produces an approximate constant force along a variable range of gripper. The mechanism is symmetric; thus, one side is considered for the analytic model. The mathematical model of this mechanism is to be created using the Pseudo-Rigid Body Method. The parameters of the mathematical model are calculated analytically and then optimized to obtain a constant force gripper. Finally, this mechanism is analyzed by finite element method and compared with the mathematical model.

Keywords: Compliant Mechanism, Constant Force Compliant Gripper Mechanism, Pseudo-Rigid Body Method, Virtual Work Principle, Finite Element Analysis

ÖZET

SABIT KUVVETLİ ÖZGÜN BİR ESNEK TUTUCU TASARIMI

Mehmet Oğuz ÖZTÜRK

Yüksek Lisans, Makine Mühendisliği Bölümü

Tez Danışmanı: Prof. Dr. Volkan PARLAKTAŞ

Eş Danışman: Prof. Dr. Engin TANIK

Nisan 2023, 64 sayfa

Bu tezin amacı, sabit kuvvetli özgün bir tutucu mekanizması tasarlamaktır. Tasarım, bir tarafı sabit, tutucu tarafı serbest olan yekpare bir tutma mekanizmasıdır. Mekanizma dört esnek mafsala sahiptir ve değişken bir kısaç aralığı boyunca yaklaşık sabit bir kuvvet üretir. Mekanizma simetriktir; bu nedenle analitik model için bir taraf dikkate alınır. Bu mekanizmanın matematiksel modeli Pseudo-Rigid Body Method kullanılarak oluşturulur. Matematiksel modelin parametreleri analitik olarak hesaplanır ve daha sonra sabit kuvvetli bir kısaç elde etmek için optimize edilir. Son olarak, bu mekanizma sonlu elemanlar yöntemi ile analiz edilmiş ve matematiksel model ile karşılaştırılmıştır.

Anahtar Kelimeler: Esnek Mekanizma, Sabit Kuvvetli Esnek Kısaç Mekanizması, Sahte Rijit Cisim Metodu, Sanal İş Prensibi, Sonlu Elemanlar Analizi

ACKNOWLEDGEMENTS

Firstly, I would like to express my gratitude to my supervisor Prof. Dr. Volkan PARLAKTAŞ, and my co-supervisor Prof. Dr. Engin TANIK, for their encouragement, guidance and supervision. I complete this study with the help of them.

Also, I would like to give my sincere thanks to Dr. Çağıl Merve TANIK for her support.

Finally, I would like to give my sincere thanks to my wife, Gözde ÖZTÜRK, for her moral support, patience and love.

Mehmet Oğuz ÖZTÜRK

April 2023, Ankara

TABLE OF CONTENTS

ABSTRACT.....	i
ÖZET	ii
TABLE OF CONTENTS.....	v
FIGURES.....	vii
TABLES	ix
ABBREVIATIONS	x
1. INTRODUCTION	1
1.2. Literature Review	2
2. BACKGROUND	8
2.1. Mechanism.....	8
2.1.1. Degrees of Freedom.....	8
2.2. Compliant Mechanism.....	8
2.3. Pseudo – Rigid Body Model.....	9
2.4. Virtual Work.....	11
2.5. Constant Force	11
3. THE DESIGN MODEL OF THE CONSTANT FORCE COMPLIANT MECHANISM	13
3.1. Mathematical Model of the Mechanism	13
3.2. Calculation and Control of the Mathematical Model	17
3.2.1. Calculation and Control of the Mathematical Model with Assumption.....	17
4. Verification of The Mathematical Model	23
4.1. Selection of The Ansys Module and Material	23
4.2. Geometry Model.....	25
4.3. Generating Model of the Mechanism	28
4.4. Solutions of the Mechanism	32
5. CONCLUSION.....	37
REFERANCES.....	39

APPENDIX	41
Appendix 1 – The Design Codes.....	41
CURRICULUM VITAE	43

FIGURES

Figure 1: Movable and compliant joints [2].	1
Figure 2: Concept compliant gripper mechanism design.	2
Figure 3: Rigid (a) and compliant arm-slider mechanism (b) [3].	3
Figure 4: Compliant constant-force mechanism [5].	3
Figure 5: A slider-crank gripper with kinematic diagram (a) and rigid-body counterpart (b) [6].	4
Figure 6: A compliant dual-axis gripper [7].	5
Figure 7: Partially compliant variable stroke mechanism [8].	5
Figure 8: Compliant constant-force linear-motion mechanism [13].	6
Figure 9: Different grasping objects grouped in the three main grasping patterns. [14].	6
Figure 10: Rigid body of the mechanism [15].	7
Figure 11: Compliant remote center of motion mechanism [16].	7
Figure 12: Compliant slider-crank mechanism [1].	9
Figure 13: Compliant mechanism (a) its PRBM (b) [1].	10
Figure 14: PRBM (a) the mechanism with fixed guided compliant segments (b) [18].	10
Figure 15: Ideal force and deflection diagram [15].	11
Figure 16: Desired F-D diagram [15].	12
Figure 17: Actual F-D curve [15].	12
Figure 18: The design model of the compliant gripper.	13
Figure 19: The symmetry model of the compliant gripper.	13
Figure 20: The PRBM of the compliant gripper.	14
Figure 21: Free-Body diagram of the mechanism.	18
Figure 22: Sketch analysis of the mechanism.	20
Figure 23: Theta 2 values of the mechanism.	21
Figure 24: Theta 3 values of the mechanism.	21
Figure 25: Constant-Force graph of the gripper mechanism.	22
Figure 26: Engineering data and static structural module.	24
Figure 27: Properties of the material.	24
Figure 28: Ansys project table.	25
Figure 29: PRBM of the mechanism.	26
Figure 30: Geometry model of the mechanism.	27
Figure 31: Detail of the mechanism.	27
Figure 32: Importing the 3D model.	28
Figure 33: Material selection.	29
Figure 34: Meshing of the mechanism.	29
Figure 35: Mesh detail.	29
Figure 36: Analysis settings.	30
Figure 37: Fixed support of the mechanism.	31
Figure 38: Contacts of the links and hinges.	31

Figure 39: Applying remote displacement..... 32
Figure 40: Selection of the displacement point..... 32
Figure 41: Solutions of the mechanism..... 33
Figure 42: Force converge diagram of the mechanism..... 33
Figure 43: Force reaction solution of the mechanism..... 34
Figure 44: Comparison of the mechanism..... 35
Figure 45: Equivalent stress of the mechanism..... 36
Figure 46: Detailed equivalent stress a) First Hinge b) Second Hinge 36

TABLES

Table 1: Dimension of the optimized mechanism.	20
Table 2: The properties of the material.	23
Table 3: Dimension of the mechanism.	26

ABBREVIATIONS

DOF	Degree of Freedom
PRBM	Pseudo Rigid Body Model
CM	Compliant Mechanism
CFMs	Constant Force Mechanisms
CFCGM	Constant Force Compliant Gripper Mechanism
FBD	Free Body Diagram
MEMS	Micro Electro Mechanical Systems
RM	Rigid Member
FM	Flexural Member
LD	Large Deflection

1. INTRODUCTION

In engineering, mechanism is defined as a mechanical device that has movable joints, consists of several links, one of which is fixed, and transfers or transforms inputs such as force, movement or energy into a desired set of output force, movement or energy. Accordingly, a compliant mechanism is described that transmits or converts force, movement or energy exactly like classical mechanism. Unlike rigid-link mechanisms, compliant mechanisms fulfill their transfer and transformation functions as well by deflection of flexible members rather than movable joints only [1].

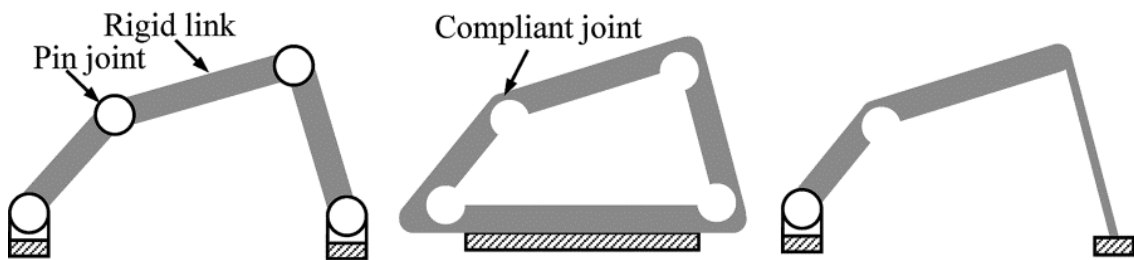


Figure 1: Movable and compliant joints [2].

The main purpose of the study is to design, analyze and manufacture a novel and multi-purpose compliant constant force gripper mechanism using Pseudo Rigid Body Model (PRBM) technique. The novel design is a monolithic holding mechanism which is fixed on one side and free on the gripper side as shown in Fig.3. Accordingly, the mechanism has four compliant hinges and produces an approximate constant force along a variable range of the gripper. Also, the mechanism is symmetric; thus, one side is considered for the analytic model. The parameters of the mathematical model are calculated analytically and then optimized to obtain a constant force gripper. Consequently, this mechanism is analyzed by finite element method and compared with the mathematical model.

In this context, PRBM is an approximation technique for modelling a compliant mechanism, especially for those where the compliant joints experience large deflection and leads to non-linear behavior [1]. So, the purpose of using the PRBM technique is that it actual becomes a bridge between classical rigid-body mechanism theory and compliant mechanism analysis. Also, the design steps are; (i) type determination; the novel preliminary design is sketched (Figure 2), (ii) the PRBM of the compliant mechanism is obtained, (iii) analytical model is determined by using the PBRM, (iv) mechanism

dimensions are optimized to obtain an approximate constant force mechanism, (v) determine mechanisms are also analyzed by FEA and results are compared.

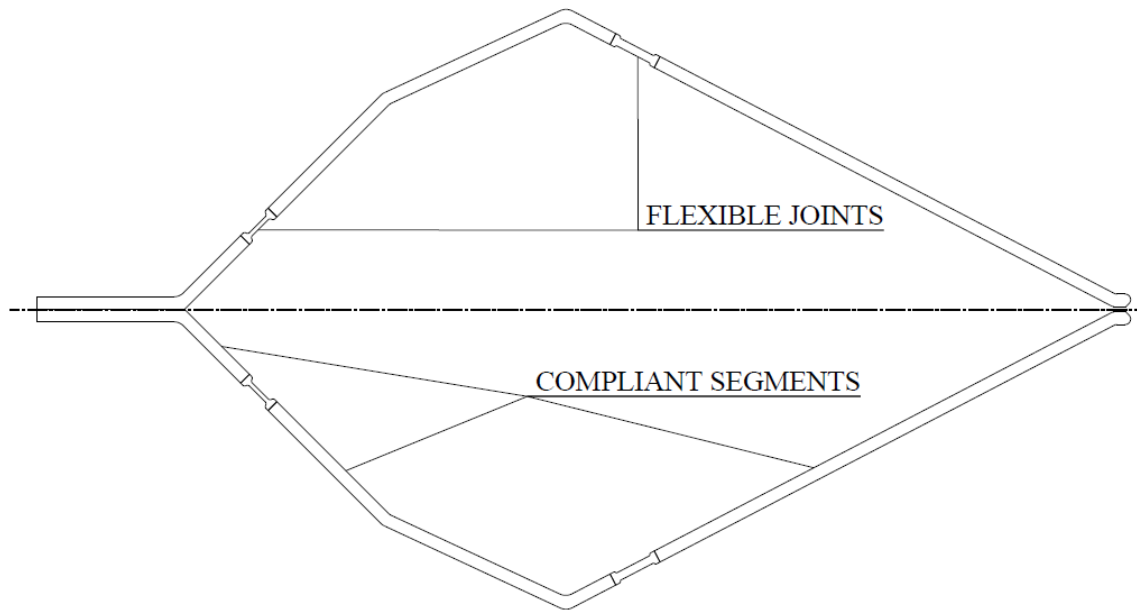


Figure 2: Concept compliant gripper mechanism design.

The fully compliant constant force gripper is a simple and inexpensive alternative to the existing robot gripper solutions especially vital for biotechnology or MEMS applications.

1.2. Literature Review

Recent research shows that; compliant mechanisms provide advantages in two very important categories when compared to classical mechanisms. The first of these advantages is that it reduces the cost as it decreases the number of the parts of the mechanism, assembly time and simplifies the manufacturing method like figure 3 [3]. Secondly, since the movable joints are not used, there are no factors that negatively affect the mechanism such as wear, weight and maintenance. Therefore, the mechanism is both cheaper and simplified. Accordingly, using area of the compliant mechanism like compliant micro gripper [4] has become widespread in important sectors such as Biotechnology and Micro-Electro-Mechanic Systems (MEMS), as well as industrial products, for example, shampoo caps, backpack latch or wiper that can be seen readily in daily life.



Figure 3: Rigid (a) and compliant arm-slider mechanism (b) [3].

Although having a lot of advantages, compliant mechanisms have some difficulties and disadvantages. The analysis and design of compliant mechanisms is one of its most important disadvantages. Because a flexible joint is used instead of a movable joint, the mathematical equations used in rigid-link mechanisms are not valid. So, in order to overcome this challenge, Pseudo-Rigid-Body-Model (PRBM) which is explained in the following pages is used in the designing of the compliant mechanism (Figure 4). In addition, the energy storage feature of the flexible joints is an important advantage as it simplifies the mechanism, nevertheless, when the input energy is wished to be transferred to output energy by the mechanism, it turns into a disadvantage since some of the energy is stored in the mechanism. Besides, fatigue analysis of the material, rotational limit of the deformable joints and stress relaxation or creep of compliant links under stress for a long time are critically crucial for compliant mechanisms.

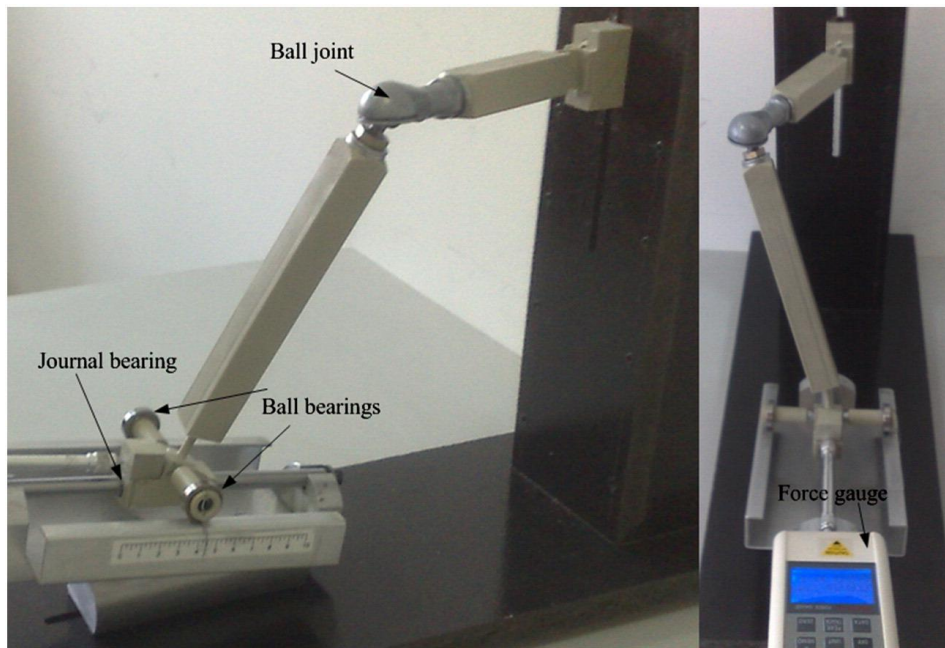


Figure 4: Compliant constant-force mechanism [5].

Taking into the account the recent developments in the field of robotics and electronics industry, it is observed that the tremendous demand and requirement for grippers have been increased. However, these gripper mechanisms are complicated and costly as conventional force-controlled mechanisms require the use of force sensors and controllers. Therefore, constant-force compliant mechanisms (CFCMs) are arousing considerable interest to avoid this complex design and cost (Figure 5).

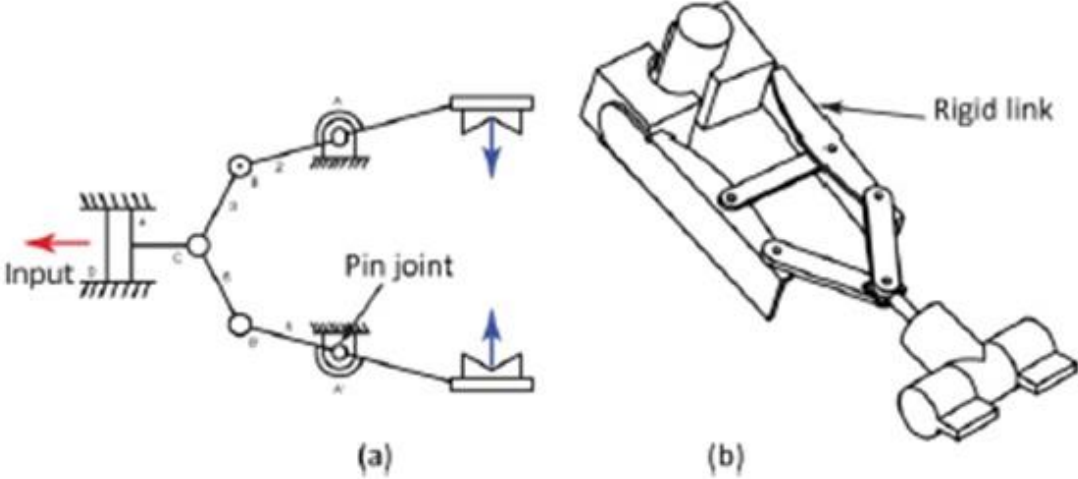


Figure 5: A slider-crank gripper with kinematic diagram (a) and rigid-body counterpart (b) [6].

When the recent studies on constant-force compliant mechanisms are examined, in the first place, it is comprehended that the relationships between input force and displacement are investigated. [7, 8, 9, 10, 11, 12] Because, regardless of whether input force constant or variable, input displacement is desired to be as high level as possible such as figure 6 and 7. Hence, joints, topology and structural analysis of compliant mechanism become significant.

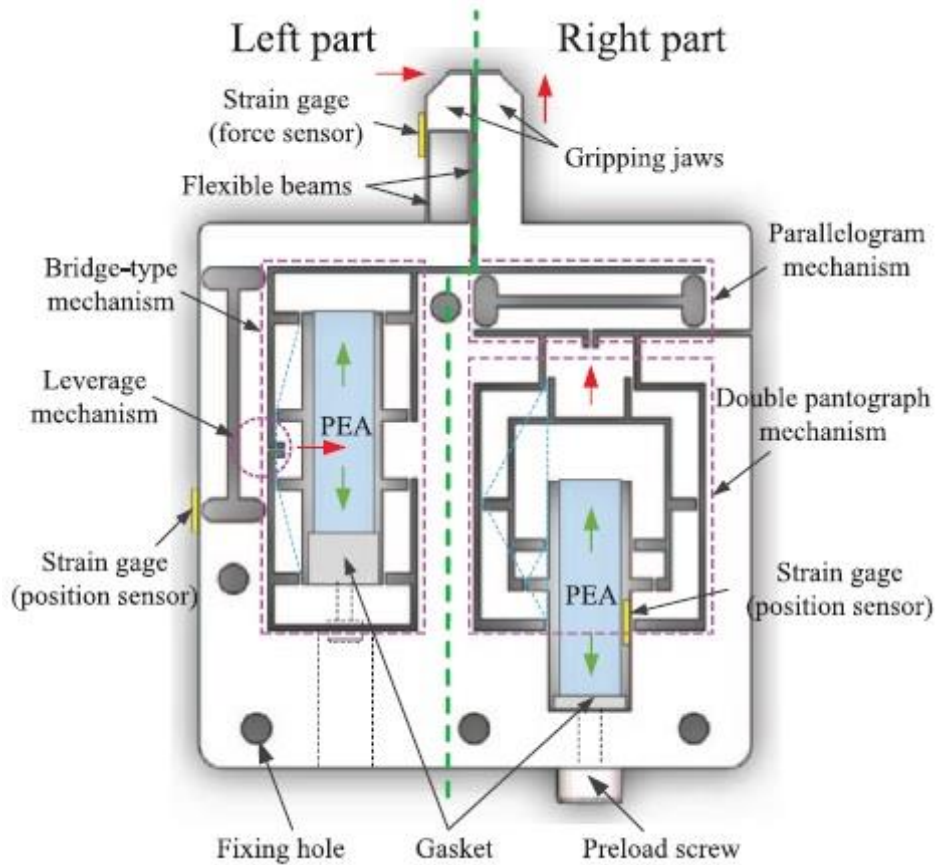


Figure 6: A compliant dual-axis gripper [7].

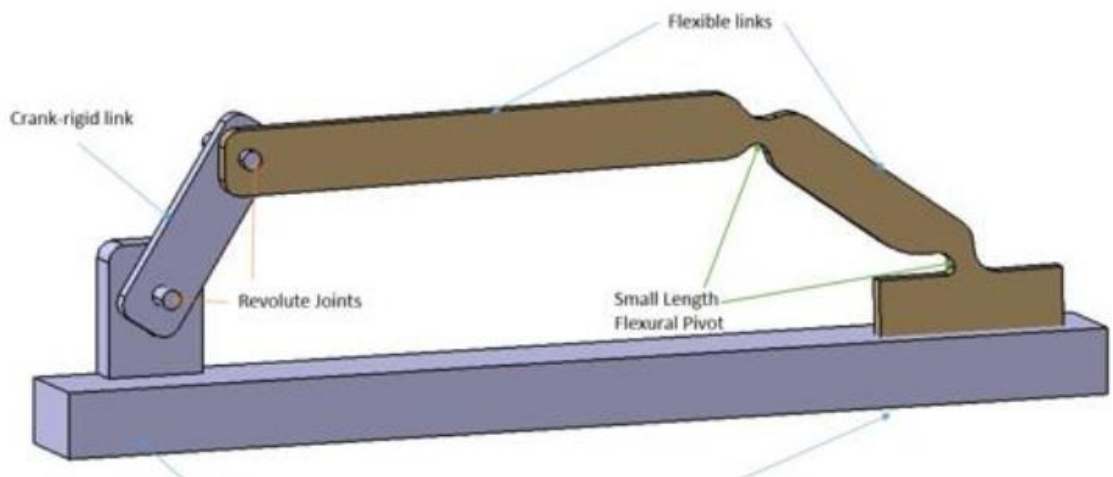


Figure 7: Partially compliant variable stroke mechanism [8].

Secondly, the studies conducted are related to manipulation of compliant mechanisms [13, 14] in figures 8 and 9. Especially, if biotechnology and micro electro mechanical systems (MEMS) are taken into consideration, the manipulations should be at the level of micrometers and ensure stability and rigidity such as figure 10 and 11. Also, the studies done are about the determination and recognition of the shapes of the

objects to be grasped [15, 16, 17, 18]. In these studies, compliant grippers detect the shape of the objects by means of embedded sensors as part of their structure.



Figure 8: Compliant constant-force linear-motion mechanism [13].

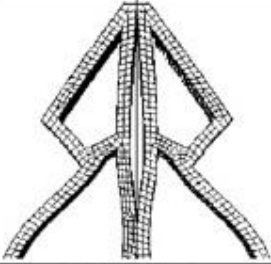
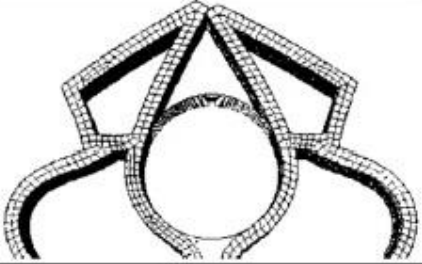
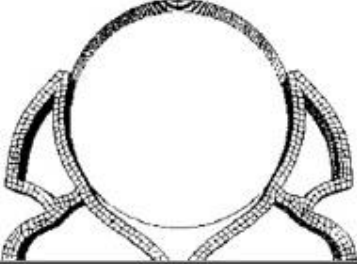
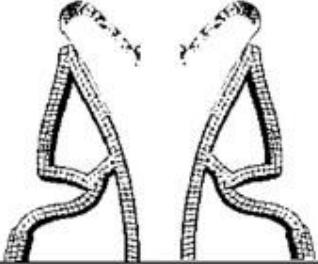
	
No object	Convex
	
Convex	Concave

Figure 9: Different grasping objects grouped in the three main grasping patterns. [14].

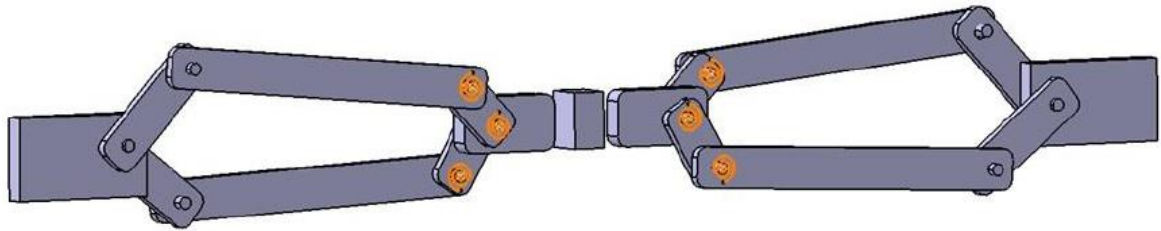


Figure 10: Rigid body of the mechanism [15].

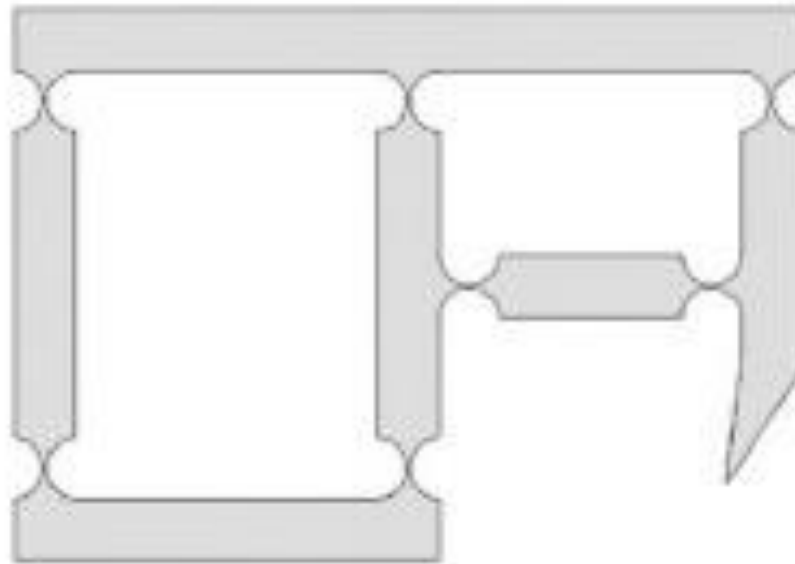


Figure 11: Compliant remote center of motion mechanism [16].

2. BACKGROUND

2.1. Mechanism

A mechanism, in the most general sense, may be defined as a system in which links are connected with joints for the transmission of motion, force or energy. So, while the mechanisms fulfill their designated functionality, it is assumed that their fasteners are rigid. Therefore, the degrees of the freedom of the joints of the mechanisms and their relative motion with respect to each other are a distinctive feature of the conventional mechanisms.

2.1.1. Degrees of Freedom

The degrees of the freedom of a mechanism may be defined as the minimum number of the variables required to determine the position of the links of that mechanism. Accordingly, a general formula called as Gruebler's Equation is given below to calculate the degrees of the freedom of a mechanism.

$$F = \lambda(l - j - 1) + \sum_{i=1}^j f_i \quad (2.1)$$

$\lambda =$ Degree of Freedom of Space; $\lambda = 3$ for Planar space, 6 for general space,

$l =$ Number of the links in a mechanism (including the fixed link),

$j =$ Number of the joints in a mechanism,

$f_i =$ The degree of freedom of the i th joint in a mechanism,

$F =$ The degree of freedom of the mechanism

2.2. Compliant Mechanism

Compliant mechanism may be described as a mechanism transmits a motion, force or energy like traditional mechanism. While the traditional mechanisms complete their functionality with the help of the joints, the compliant mechanisms fulfill this process by using flexible members. Therefore, the compliant mechanism is a flexible mechanism which exhibits elastic behavior and works under load. So, deflection, stiffness, stress and properties of the material are quite vital for compliant mechanism. For this reason, analyzing the compliant mechanism is very difficult and complex. Also, while the

analysis is run, it is necessary to calculate the force to produce the deflection and stress as the deflection is known like figure 10.

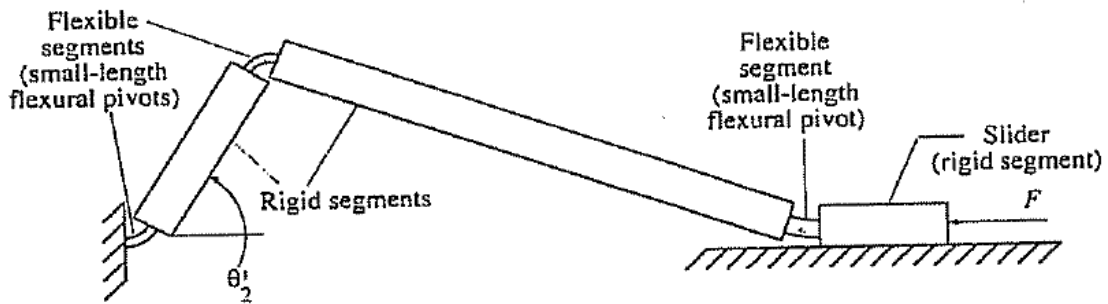


Figure 12: Compliant slider-crank mechanism [1].

2.3. Pseudo – Rigid Body Model

There are a lot of effective way to design a mechanism by using large deflection analysis methods. But in these methods, it is needed initial parameters such as geometry, material properties and load conditions in order to calculate the algorithm of the mechanism. Therefore, there is more effective method for compliant mechanism called as Pseudo-Rigid Body Model (PRBM). Also, in this method it is aimed that analyzing the mechanism undergoes large and nonlinear deflections in a simple way. *“The pseudo rigid-body model concept is used to model the deflection of flexible members using rigid-body components that have equivalent force-deflection characteristics”* [1]. Thus, it must be calculated the deflection path and force-deflection relationships of a flexible member for every flexible member in the mechanism. For this reason, main point of this method is to determine where to set the pin joints and what value to designate the spring constant such as figure 13 and 14.

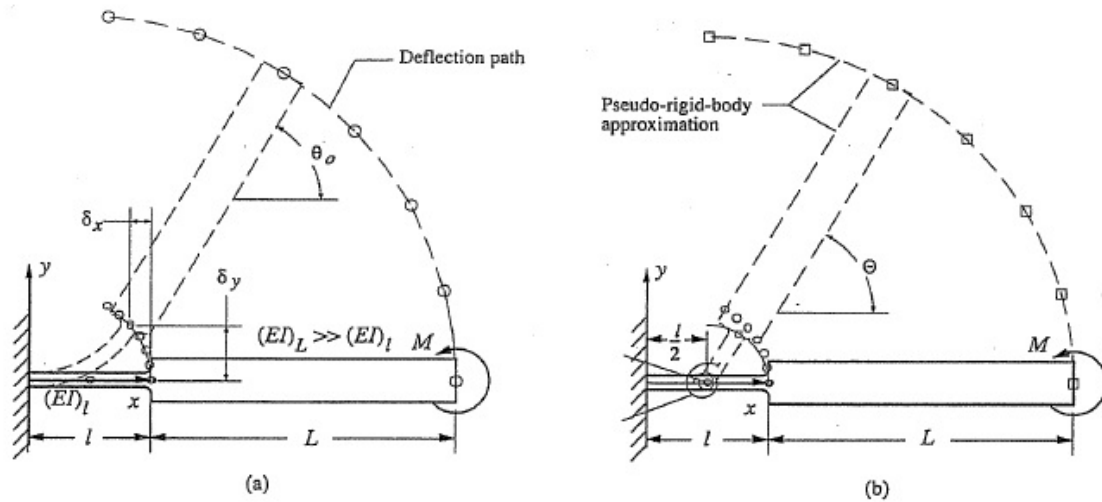


Figure 13: Compliant mechanism (a) its PRBM (b) [1].

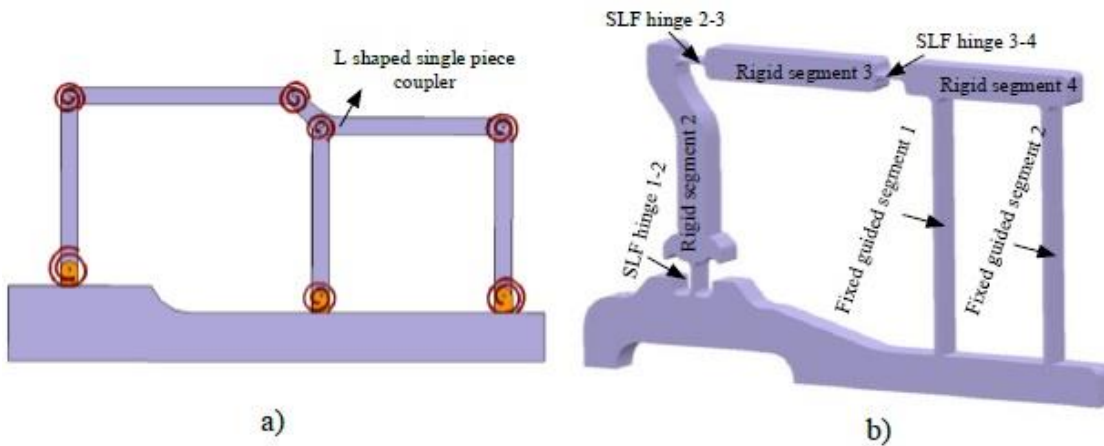


Figure 14: PRBM (a) the mechanism with fixed guided compliant segments (b) [18].

To design a compliant mechanism with PRBM, there are some approximation values such as characteristic radius factor, stiffness coefficient and parameterization limit. Therefore, using the average of the approximation values, a compliant mechanism may be calculated with a small margin of error.

2.4. Virtual Work

If a force is applied to a mechanism which rigid links are connected to each other by movable joints or flexible joints, there are two ways to calculate the reaction forces at the joints. The first one of these methods is the free-body diagram approach, in which the reaction forces are calculated by drawing the free body diagram of all members. The second one is the virtual work method. In this method, calculating all reaction forces are not necessary. So, using the virtual work method with is prevalent.

2.5. Constant Force

There are a lot of applications which gripping force is vital such as MEMS and biotechnology. So, a constant force mechanism is needed that there is no change in output force regardless of input force. Accordingly, in figure 15 it is comprehended that there is a relationship between applied force (F) and resulted displacement (D) in terms of performance.

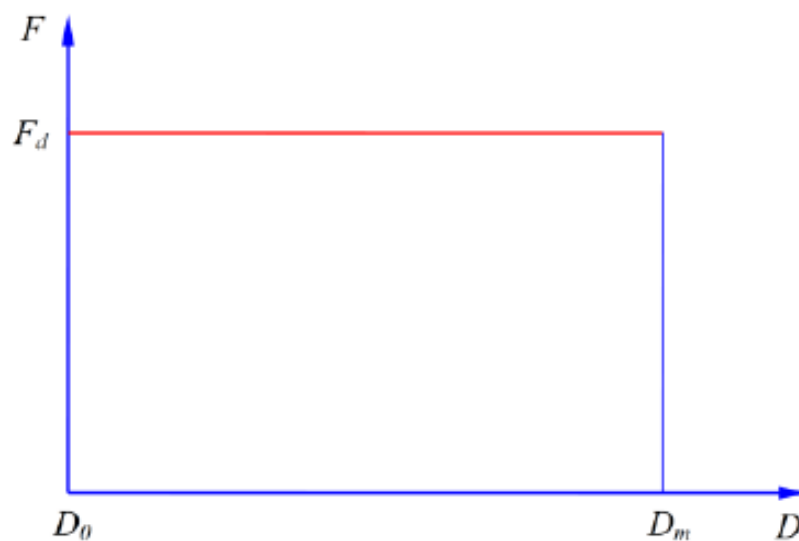


Figure 15: Ideal force and deflection diagram [15].

In ideal F-D diagram it is inferred that F-D curve represents the stiffness of the material and stiffness is zero because of unchanged the force.

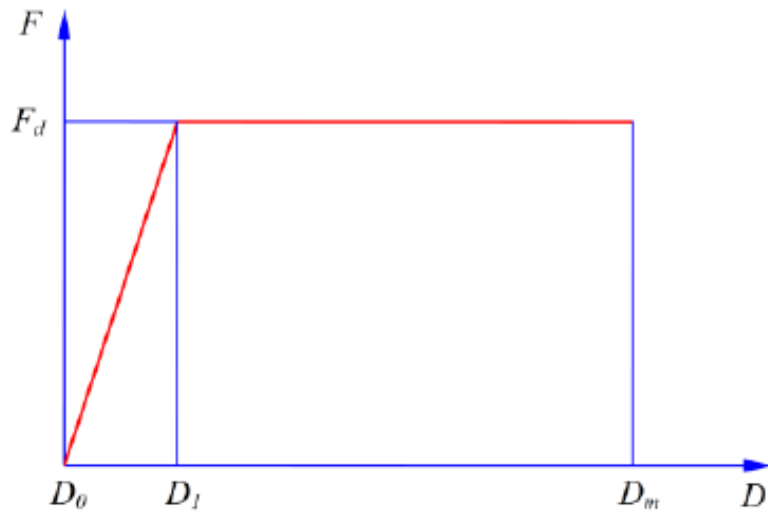


Figure 16: Desired F-D diagram [15].

In figure 16, it is shown that if a force is not applied, a displacement is not resulted, that is the ideal F-D curve is impossible. Hereby, desired constant force is taken place between D_1 and D_m .

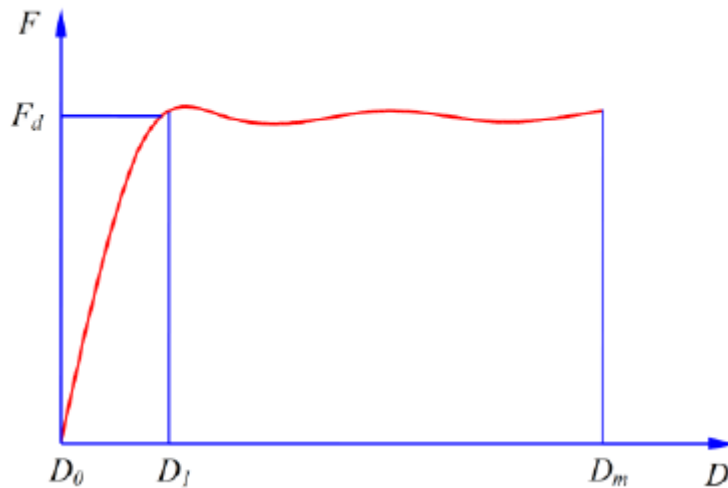


Figure 17: Actual F-D curve [15].

In the actual constant force compliant mechanisms, force fluctuates like shown in the figure 17 between D_1 and D_m . So, it is aimed that fluctuating of the force is minimized or reduced.

3. THE DESIGN MODEL OF THE CONSTANT FORCE COMPLIANT MECHANISM

3.1. Mathematical Model of the Mechanism

In this study, it is proposed a novel constant force gripper based on a fully compliant single piece mechanism. And, this mechanism has five rigid segments connected with four flexible joints each other shown in figure 18. Also, it is aimed that the compliant gripper produces approximate constant force to provide sensitive grasp. So, when all these purposes are considered, the length of the links and the spring constant ratio of the flexible joints are studied to maximize the constant force range and minimize the constant force fluctuating.

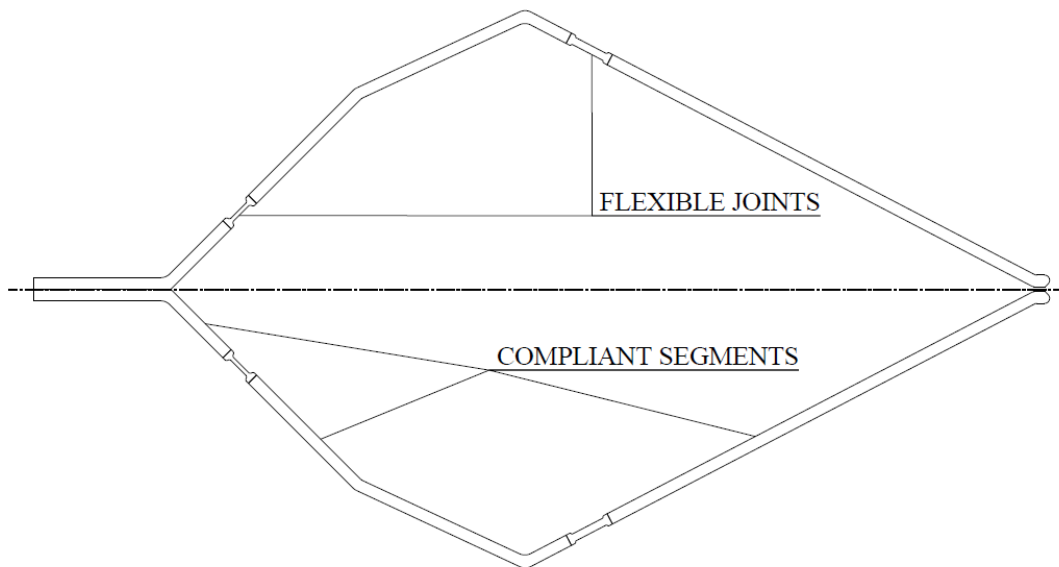


Figure 18: The design model of the compliant gripper.

Since the created design model is symmetry, the upper-half of the design model is investigated for convenience of analysis (Figure 19).

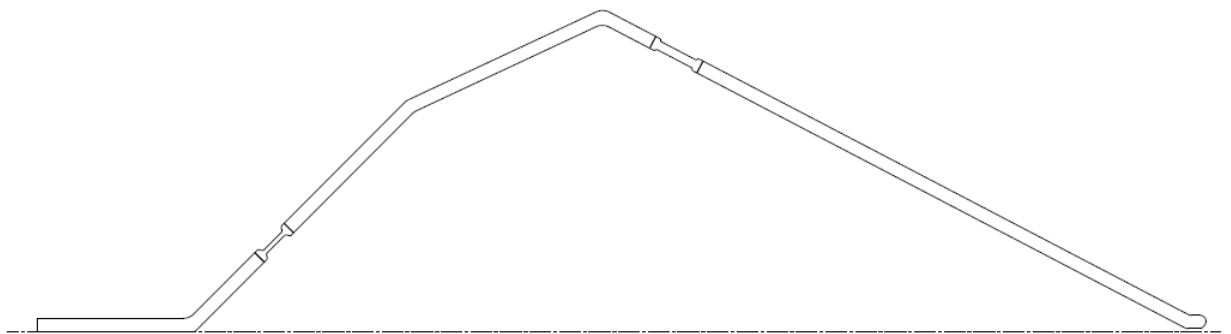


Figure 19: The symmetry model of the compliant gripper.

The design model is adapted to the PRBM model so that it can be examined as compliant mechanisms (Figure 20).

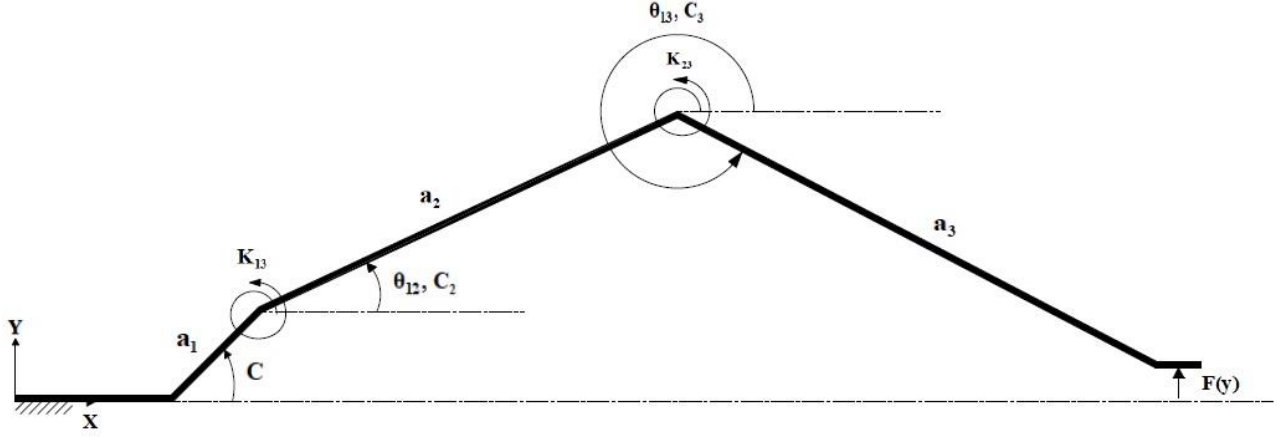


Figure 20: The PRBM of the compliant gripper.

Firstly, loop closure equations with links a_1 , a_2 , and a_3 are generated in order to derive the relevant mathematical equations of the compliant gripper mechanism for which the PRBM design model is created.

$$a_1 e^{ic} + a_2 e^{i\theta_{12}} + a_3 e^{i\theta_{13}} = x + iy \quad (3.1)$$

$$a_1 \cos c + a_2 \cos \theta_{12} + a_3 \cos \theta_{13} = x \quad (3.2)$$

$$a_1 \sin c + a_2 \sin \theta_{12} + a_3 \sin \theta_{13} = y \quad (3.3)$$

Differentiating the equations 3.2 and 3.3;

$$\delta x = -a_2 \sin \theta_{12} \delta \theta_{12} - a_3 \sin \theta_{13} \delta \theta_{13} \quad (3.4)$$

$$\delta y = a_2 \cos \theta_{12} \delta \theta_{12} + a_3 \cos \theta_{13} \delta \theta_{13} \quad (3.5)$$

If the 3.4 and 3.5 equations are rearranged with respect to $\delta \theta_{12}$ and $\delta \theta_{13}$;

$$\delta \theta_{12} = \frac{-\delta x - a_3 \sin \theta_{13} \delta \theta_{13}}{a_2 \sin \theta_{12}} \quad (3.6)$$

$$\delta \theta_{13} = \frac{\delta y - a_2 \cos \theta_{12} \delta \theta_{12}}{a_3 \cos \theta_{13}} \quad (3.7)$$

Thus, the closed loop equations of the constant force gripper mechanism are derived.

If the constant force compliant gripper mechanism is adapted according to the virtual work principle, the sum of all the work-producing elements of the mechanism in static equilibrium will be equal to zero.

$$\delta w_{total} = \delta w_{internal} + \delta w_{external} = 0 \quad (3.8)$$

As external work, there is only the force F on the y-axis.

$$\delta w_{external} = F_y \delta y \quad (3.9)$$

As the internal force, there are two torsional springs, which are the PRBM counterparts of flexible joints. K_{12} and K_{23} are spring force constant of the mechanism. Also, C_2 and C_3 are the initial angle of the theta 2 and theta 3 respectively.

$$\delta w_{internal} = \delta w_{springs2} + \delta w_{springs3} \quad (3.10)$$

$$\delta w_{springs2} = - \left[\frac{d \left(\frac{1}{2} K_{12} (\theta_{12} - C_2)^2 \right)}{d \theta_{12}} \right] \delta \theta_{12} \quad (3.11)$$

$$\delta w_{springs2} = -K_{12} (\theta_{12} - C_2) \delta \theta_{12} \quad (3.12)$$

$$\delta w_{springs3} = - \left[\frac{d \left(\frac{1}{2} K_{23} (\theta_{13} - \theta_{12} + C_2 - C_3)^2 \right)}{d \theta_{13}} \right] \delta \theta_{12} \quad (3.13)$$

$$\delta w_{springs3} = -K_{23} (\theta_{13} - \theta_{12} + C_2 - C_3) \left(\frac{\delta \theta_{13}}{\delta \theta_{12}} - 1 \right) \delta \theta_{12} \quad (3.14)$$

$$\delta w_{springs3} = -K_{23} (\theta_{13} - \theta_{12} + C_2 - C_3) (\delta \theta_{13} - \delta \theta_{12}) \quad (3.15)$$

$$\delta w_{internal} = -K_{12} (\theta_{12} - C_2) \delta \theta_{12} - K_{23} (\theta_{13} - \theta_{12} + C_2 - C_3) (\delta \theta_{13} - \delta \theta_{12}) \quad (3.16)$$

$$\delta w_{internal} = \left[K_{23} (\theta_{13} - \theta_{12} + C_2 - C_3) - K_{12} (\theta_{12} - C_2) \right] \delta \theta_{12} - K_{23} (\theta_{13} - \theta_{12} + C_2 - C_3) \delta \theta_{13} \quad (3.17)$$

$$\delta w_{total} = F_y \delta y + \left[K_{23} (\theta_{13} - \theta_{12} + C_2 - C_3) - K_{12} (\theta_{12} - C_2) \right] \delta \theta_{12} - K_{23} (\theta_{13} - \theta_{12} + C_2 - C_3) \delta \theta_{13} \quad (3.18)$$

$$A = K_{23} (\theta_{13} - \theta_{12} + C_2 - C_3) \quad (3.19)$$

$$\delta w_{total} = F_y \delta y + [A - K_{12}(\theta_{12} - C_2)] \delta \theta_{12} - A \frac{\delta y - a_2 \cos \theta_{12} \delta \theta_{12}}{a_3 \cos \theta_{13}} \quad (3.20)$$

$$\delta w_{total} = \left(F_y - \frac{A}{a_3 \cos \theta_{13}} \right) \delta y + \left[A - K_{12}(\theta_{12} - C_2) + \frac{A a_2 \cos \theta_{12}}{a_3 \cos \theta_{13}} \right] \delta \theta_{12} \quad (3.21)$$

$$\delta w_{total} = \left(F_y - \frac{(\theta_{13} - \theta_{12} - C_3)}{a_3 \cos \theta_{13}} \right) \delta y + \left[K_{23}(\theta_{13} - \theta_{12} - C_3) - K_{12}(\theta_{12} - C_2) + \frac{K_{23}(\theta_{13} - \theta_{12} - C_3) a_2 \cos \theta_{12}}{a_3 \cos \theta_{13}} \right] \delta \theta_{12} \quad (3.22)$$

If the virtual work equation 3.22 for two DOF is solved, the terms in parentheses of δy and $\delta \theta_{12}$, must be equal to zero.

$$F_y - \frac{K_{23}(\theta_{13} - \theta_{12} + C_2 - C_3)}{a_3 \cos \theta_{13}} = 0 \quad (3.23)$$

$$K_{23}(\theta_{13} - \theta_{12} + C_2 - C_3) - K_{12}(\theta_{12} - C_2) + \frac{K_{23}(\theta_{13} - \theta_{12} + C_2 - C_3) a_2 \cos \theta_{12}}{a_3 \cos \theta_{13}} = 0 \quad (3.24)$$

In order to calculate readily the design parameters, the dimensionless formulas are derived from the 3.23 and 3.24 equations.

If the equation 3.23 is multiplied by a_3/K_{23} ;

$$F_y \frac{a_3}{K_{23}} = \frac{(\theta_{13} - \theta_{12} + C_2 - C_3)}{\cos \theta_{13}} \quad (3.25)$$

If the equation 3.24 is divided by $1/K_{23}$;

$$(\theta_{13} - \theta_{12} + C_2 - C_3) - \frac{K_{12}}{K_{23}}(\theta_{12} - C_2) + \frac{(\theta_{13} - \theta_{12} + C_2 - C_3) a_2 \cos \theta_{12}}{a_3 \cos \theta_{13}} = 0 \quad (3.26)$$

Thus, unitless design parameters are below;

$$F' = F_y \frac{a_3}{K_{23}} \quad (3.27)$$

$$R = \frac{a_2}{a_3} \quad (3.28)$$

$$K = \frac{K_{12}}{K_{23}} \quad (3.29)$$

The main dimensionless formulas are;

$$F' = \frac{(\theta_{13} - \theta_{12} + C_2 - C_3)}{\cos \theta_{13}} \quad (3.30)$$

$$(\theta_{13} - \theta_{12} + C_2 - C_3) - K(\theta_{12} - C_2) + \frac{(\theta_{13} - \theta_{12} + C_2 - C_3)a_2 \cos \theta_{12}}{a_3 \cos \theta_{13}} = 0 \quad (3.31)$$

Therefore, there are four design parameters $(K, R, \theta_{13}, \theta_{12})$.

Finally, we have four equations and four unknowns; Equations 3.2, 3.3, 3.30, and 3.31 must be solved simultaneously to obtain x , θ_2 , θ_3 , and F . Note that y is given input parameter and link lengths (a_i , spring constants K_{ij} and free positions of compliant hinges C_{ij}) are free parameters.

3.2. Calculation and Control of the Mathematical Model

For this study, the working principle of the mechanism is as follows; a displacement from zero position to final position is applied to the free end in the Y axis and due to this displacement, the θ_2 and θ_3 angles of the mechanism and free end position in the X axis changes. However, considering the physical movement of the mechanism, it moves negligibly in the X-axis. Therefore, in this study, it is assumed that the movement of the mechanism in the X-axis is constant. Thus, the mechanism that has 2DOF is reduced to 1DOF. Hence, this assumption has both simplified the mathematical model and facilitated its analysis of the mechanism. For this reason, the equations derived in the first place is to be rearranged according to the assumption that the movement of the mechanism in the X-axis is constant.

3.2.1. Calculation and Control of the Mathematical Model with Assumption

After assuming that the movement of the mechanism in the X-axis is constant, the mathematical model of the mechanism is rearranged according to the geometric principles as follows.

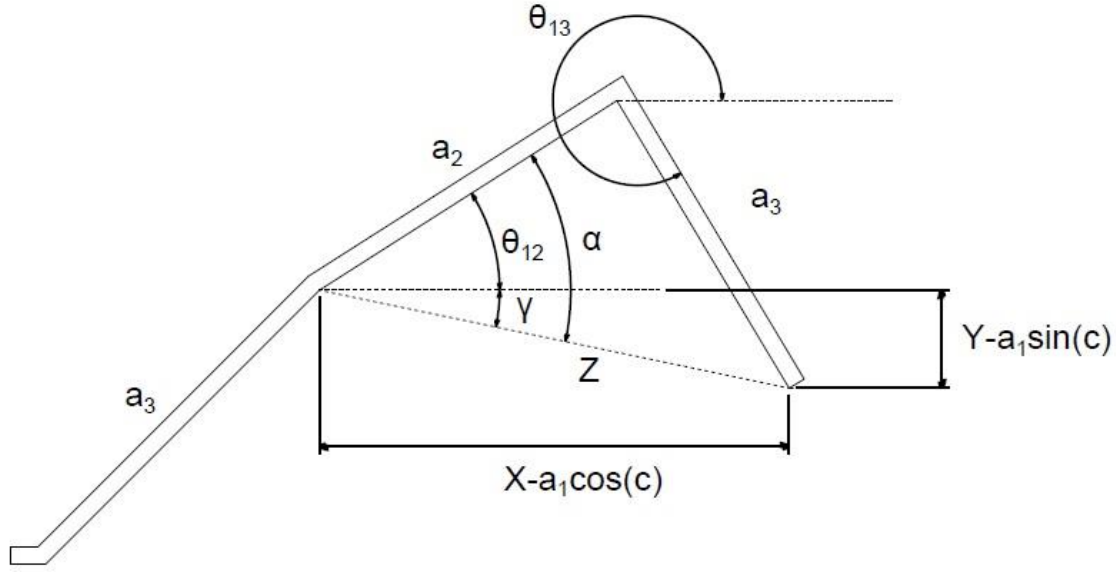


Figure 21: Free-Body diagram of the mechanism.

In order to determine the theta 2 angle in each movement of the Y, the alpha and gamma complementary angles must be determined. Therefore, the Z value is determined as shown in Figure 21.

$$Z = \sqrt{(X - a_1 \cos C)^2 + (Y - a_1 \sin C)^2} \quad (3.32)$$

$$a_3 = a_2^2 + Z^2 - 2Za_2 \cos \alpha \quad (3.33)$$

$$\alpha = a \cos \left(\frac{a_2^2 - a_3^2 + Z^2}{2Za_2} \right) \quad (3.34)$$

$$\gamma = a \tan \left(\frac{Y - a_1 \sin C}{X - a_1 \cos C} \right) \quad (3.35)$$

$$\theta_{12} = \alpha + \gamma = \alpha = a \cos \left(\frac{a_2^2 - a_3^2 + Z^2}{2Za_2} \right) + a \tan \left(\frac{Y - a_1 \sin C}{X - a_1 \cos C} \right) \quad (3.36)$$

If 3.1 and 3.2 equations rearrange for the new geometry;

$$(X - a_1 \cos C)^2 = ((a_2 \cos \theta_{12}) + (a_3 \cos \theta_{13}))^2 \quad (3.37)$$

$$(Y - a_1 \sin C)^2 = ((a_2 \sin \theta_{12}) + (a_3 \sin \theta_{13}))^2 \quad (3.38)$$

$$X^2 - 2Xa_1 \cos C + a_1^2 \cos^2 C = a_2^2 \cos^2 \theta_{12} + 2a_2a_3 \cos \theta_{12} \cos \theta_{13} + a_3^2 \cos^2 \theta_{13} \quad (3.39)$$

$$Y^2 - 2Ya_1 \sin C + a_1^2 \sin^2 C = a_2^2 \sin^2 \theta_{12} + 2a_2a_3 \sin \theta_{12} \sin \theta_{13} + a_3^2 \sin^2 \theta_{13} \quad (3.40)$$

If 3.39 and 3.40 equations sum and arrange;

$$X^2 + Y^2 - 2a_1(X \cos C + Y \sin C) + a_1^2 = a_2^2 + a_3^2 + 2a_2a_3 \cos(\theta_{12} - \theta_{13}) \quad (3.41)$$

$$\theta_{13} = \theta_{12} - a \cos\left(\frac{X^2 + Y^2 + a_1^2 - a_2^2 - a_3^2 - 2a_1(X \cos C + Y \sin C)}{2a_2a_3}\right) \quad (3.42)$$

If 3.1 and 3.2 equations derivate with respect to the new geometry for the virtual work;

$$0 = -a_2 \sin \theta_{12} d\theta_{12} - a_3 \sin \theta_{13} d\theta_{13} \quad (3.43)$$

$$\delta y = (a_2 \cos \theta_{12} d\theta_{12} + a_3 \cos \theta_{13} d\theta_{13}) \delta \theta_{12} \quad (3.44)$$

If the 3.43 and virtual works equations (3.9, 3.14) rearrange;

$$\frac{d\theta_{13}}{d\theta_{12}} = -\frac{a_2 \sin \theta_{12}}{a_3 \sin \theta_{13}} \quad (3.45)$$

$$\delta w_{external} = F_y \delta y = F_y (a_2 \cos \theta_{12} d\theta_{12} + a_3 \cos \theta_{13} d\theta_{13}) \delta \theta_{12} \quad (3.46)$$

$$\delta w_{springs3} = -K_{23} (\theta_{13} - \theta_{12} + C_2 - C_3) \left(\frac{d\theta_{13}}{d\theta_{12}} - 1 \right) \delta \theta_{12} \quad (3.47)$$

Finally, the force equation is derived from the new virtual works (3.12, 1.46, 3.47) equations as below;

$$F = \frac{K_{13} (\theta_{12} - C_2) - K_{23} (\theta_{13} - \theta_{12} + C_2 - C_3) \left(\frac{d\theta_{13}}{d\theta_{12}} - 1 \right)}{a_2 \cos \theta_{12} + a_3 \cos \theta_{13} \frac{d\theta_{13}}{d\theta_{12}}} \quad (3.48)$$

After the new equations derived from the assumption that the mechanism is constant in the X axis, a code is written in the Matlab program to calculate the position, motion and reaction force of the mechanism (Appendix 2). In addition, using this code the range in which the mechanism produces constant force is examined. Then, according to the results of this examination the constant-force compliant mechanism links are optimized (Table 1). Also, sketch analysis is fulfilled in Catia (Figure 22).

a1	11	mm
a2	10	mm
a3	9.5	mm
C	45	°
C2	32.48	°
C3	300.94 (Calculated)	°
K ₁₂	40	N*mm/°
K ₂₃	20	N*mm/°
K (K ₁₂ /K ₂₃)	2	Unitless
X	21.098 (Constant)	mm
Y	From 5 to 13	mm

Table 1: Dimension of the optimized mechanism.

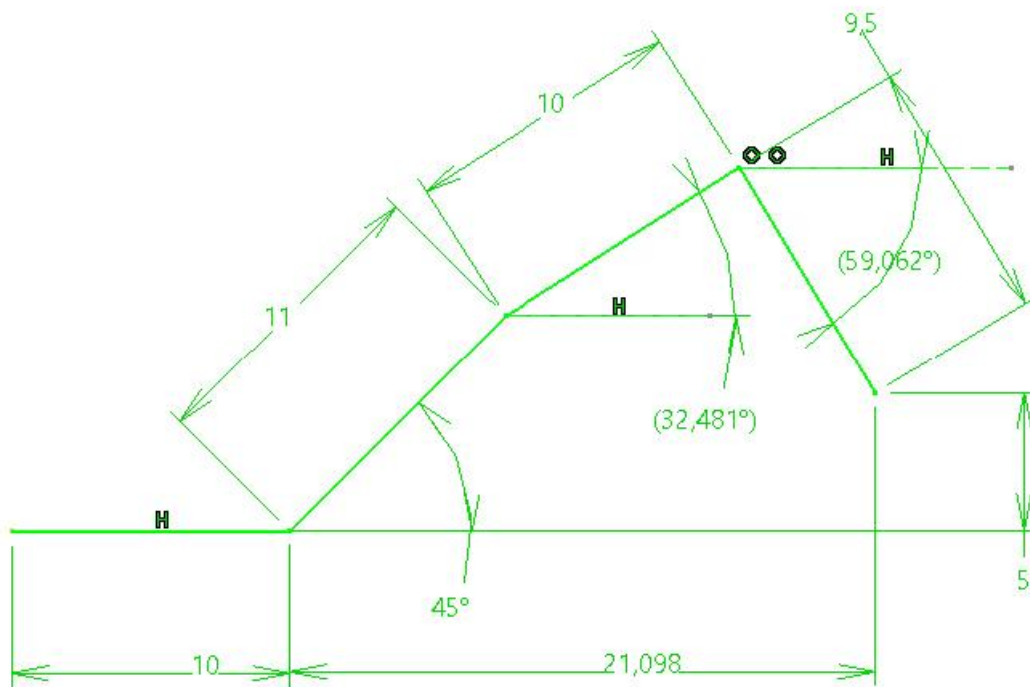


Figure 22: Sketch analysis of the mechanism.

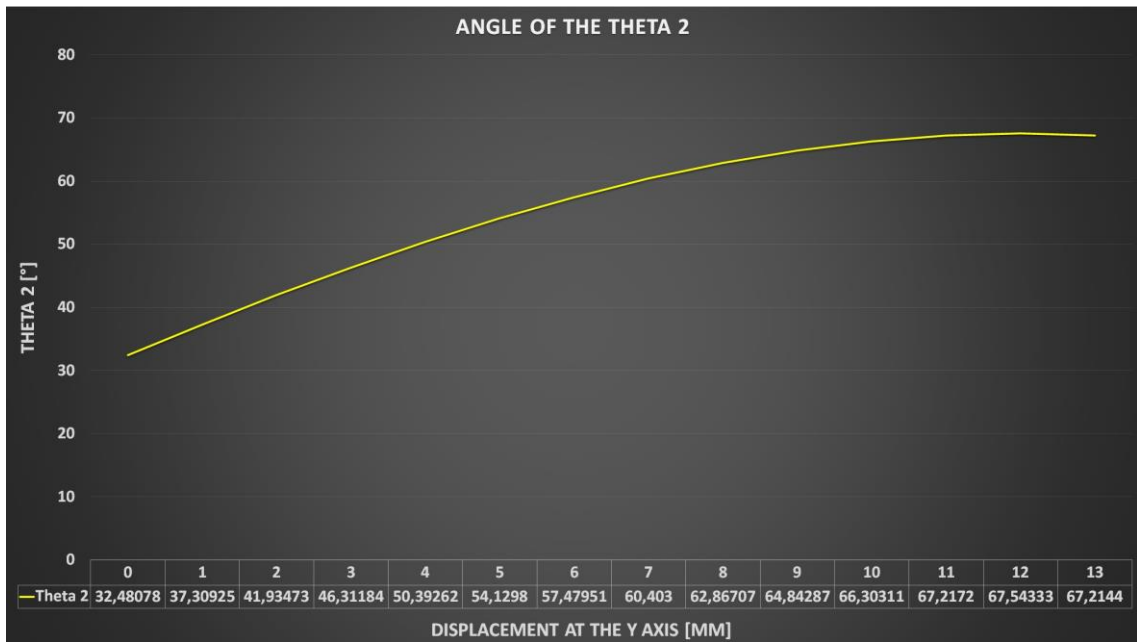


Figure 23: Theta 2 values of the mechanism.

Then, the values of the theta 2 angle corresponding to each displacement in the Y axis are calculated with the Matlab code re-written by using the optimized dimensions of the mechanism links (Figure 23).

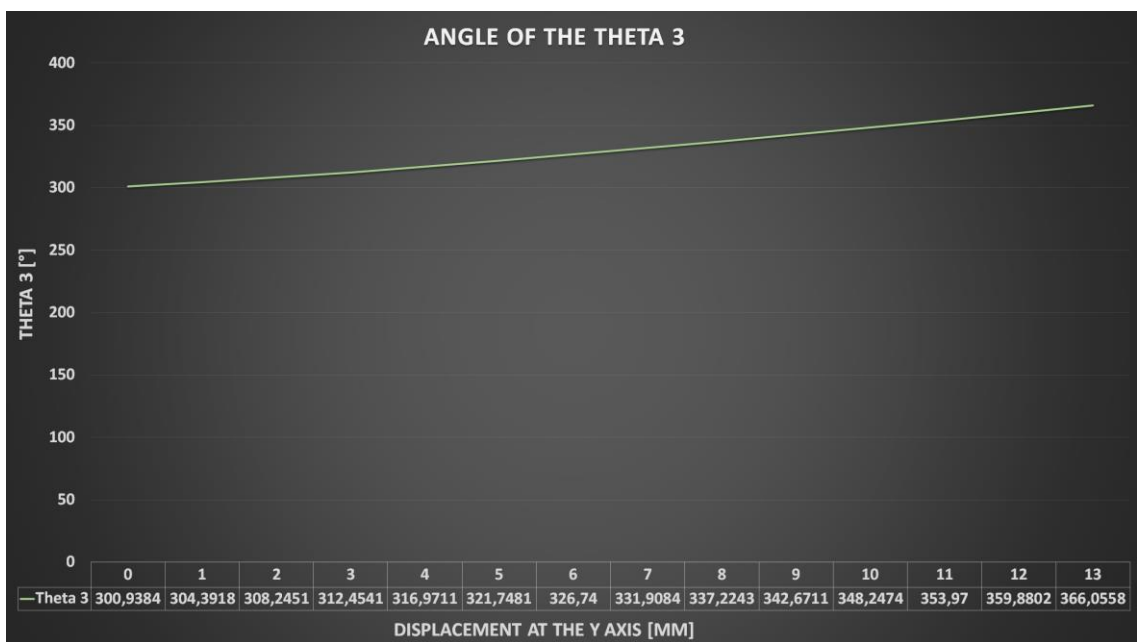


Figure 24: Theta 3 values of the mechanism.

After calculating theta 2, theta 3 data (Figure 24) is calculated for each displacement in the Y axis.

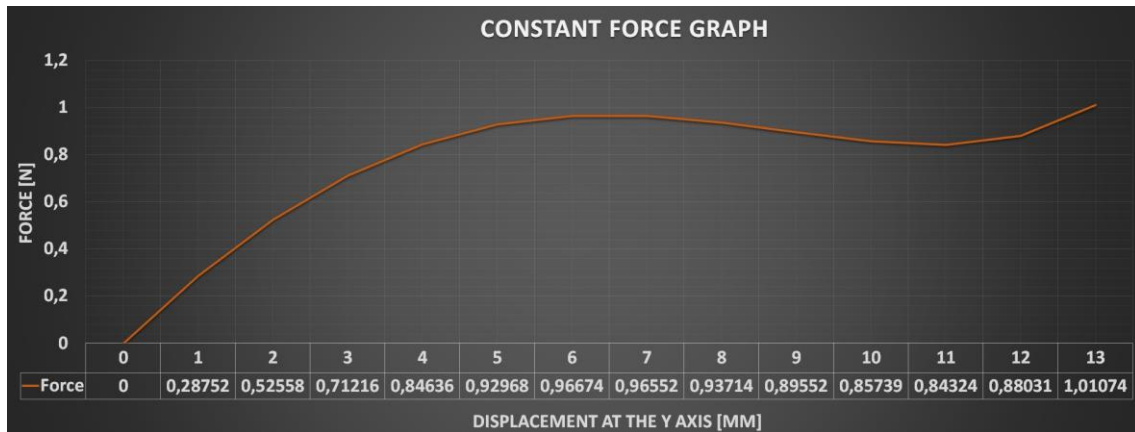


Figure 25: Constant-Force graph of the gripper mechanism.

Finally, as can be seen from Figure 25, the force is calculated for each displacement of the mechanism in the Y axis according to equation 3.48. Also, these calculations are based on the lengths of the optimized mechanism links. In this direction, if the reaction force graph (Figure 25) is interpreted, it is comprehended that the mechanism produces a constant force between the fourth step and the twelfth step. Moreover, before the fourth step, it is observed that the force produced by the mechanism fluctuates. According to the constant force theory, it is explained in detail in section 2.5 that the force will fluctuate before the mechanism produces a constant force, then oscillate quite small. When these definitions are taken into account, whether the calculated mechanism complies with the constant force theory is understood according to the percentage of oscillation. Therefore, it is converted to a percentage by averaging the force values at the point where the oscillation starts and ends. If this average value is less than 10%, the mechanism is considered to produce a constant force. Accordingly, the average force for this solution is calculated as 5.61%. So, since this value remains below 10%, it can be assumed that the mechanism produces constant force.

4. VERIFICATION OF THE MATHEMATICAL MODEL

After calculating and checking the generated mathematical model, the mechanism is validated using the Ansys Static Structural module. For this verification process, the material of the mechanism, Polypropylene, which is widely available in the market, is chosen. The properties of this material are given in Table 2 [10].

THE PROPERTIES OF THE MATERIAL		
Young's Modulus	1500	Mpa
Poisson's Ratio	0,36	Unitless
Tensile Yield Strength	35	Mpa
Compressive Yield Strength	10	Mpa
Tensile Ultimate Yield Strength	79,7	Mpa

Table 2: The properties of the material.

4.1. Selection of The Ansys Module and Material

Ansys Workbench Static Structural module is used for the verification of the mechanism in Figures 26, 27 and 28.

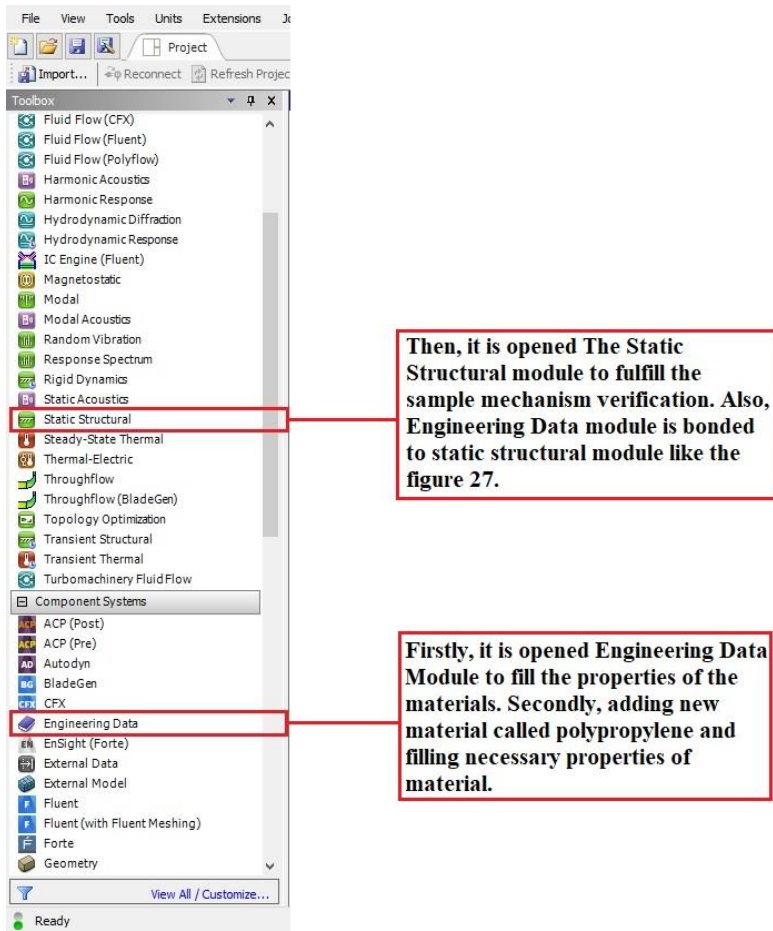


Figure 26: Engineering data and static structural module.

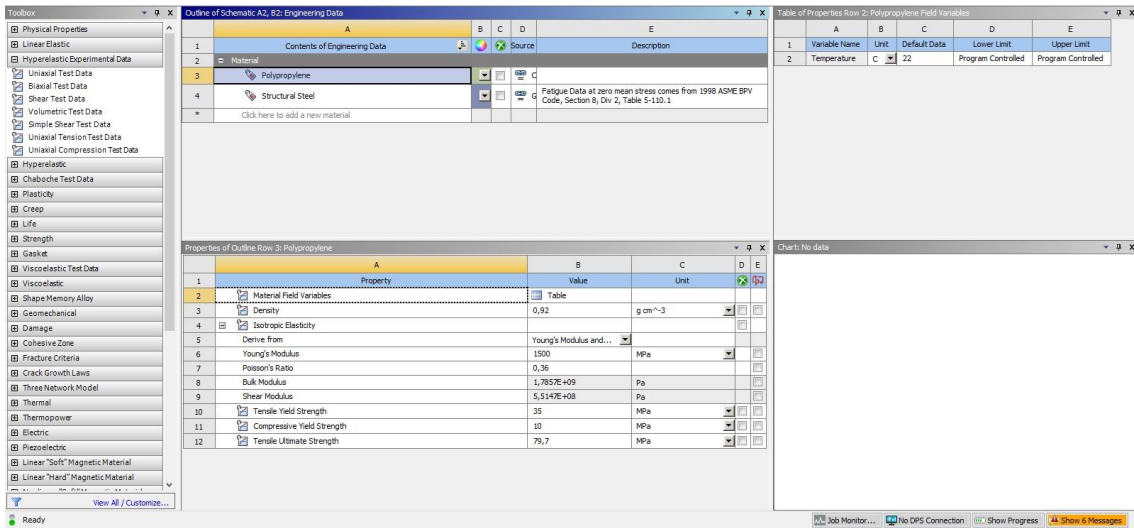


Figure 27: Properties of the material.

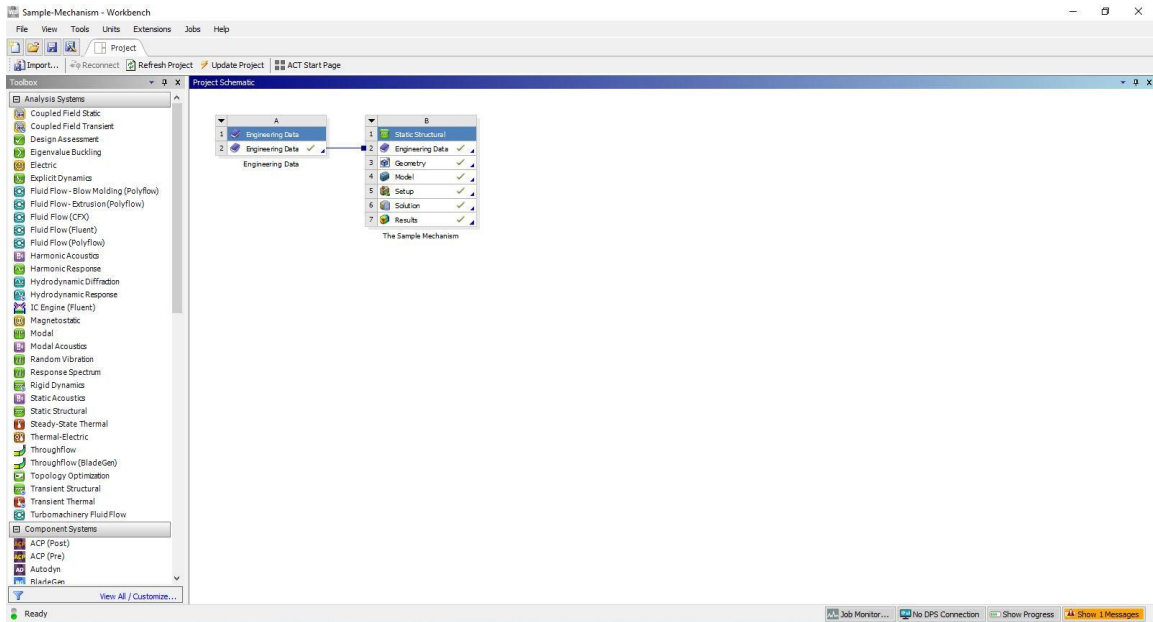


Figure 28: Ansys project table.

4.2. Geometry Model

The 3D model of the optimized mechanism is prepared using the Catia V5 R21 program. Also, this model is created in accordance with the PRBM technique (Figure 29). In addition, the optimized model is designed ten times scaled considering both its physical suitability and manufacturability. Accordingly, the ten times scaled dimensions of the created mechanism model are given in Table 3.

a1	110	mm	Length of the first link.
a2	100	mm	Length of the second link.
a3	95	mm	Length of the third link.
C	45	°	Angle of the first link.
C2	32.48	°	Angle of the second link.
K ₁₂	40	N*mm/°	Spring constant of the first hinge.
K ₂₃	20	N*mm/°	Spring constant of the second hinge.
K (K ₁₂ /K ₂₃)	2	Unitless	Spring constant ratio of the mechanism.
h	4	mm	Height of the mechanism.
h2	3,374	mm	Thickness of the first hinge.
h3	2,678	mm	Thickness of the second hinge.
l2	12	mm	Length of the first hinge.
l3	12	mm	Length of the second hinge.
w	10	mm	Width of the mechanism.

Table 3: Dimension of the mechanism.

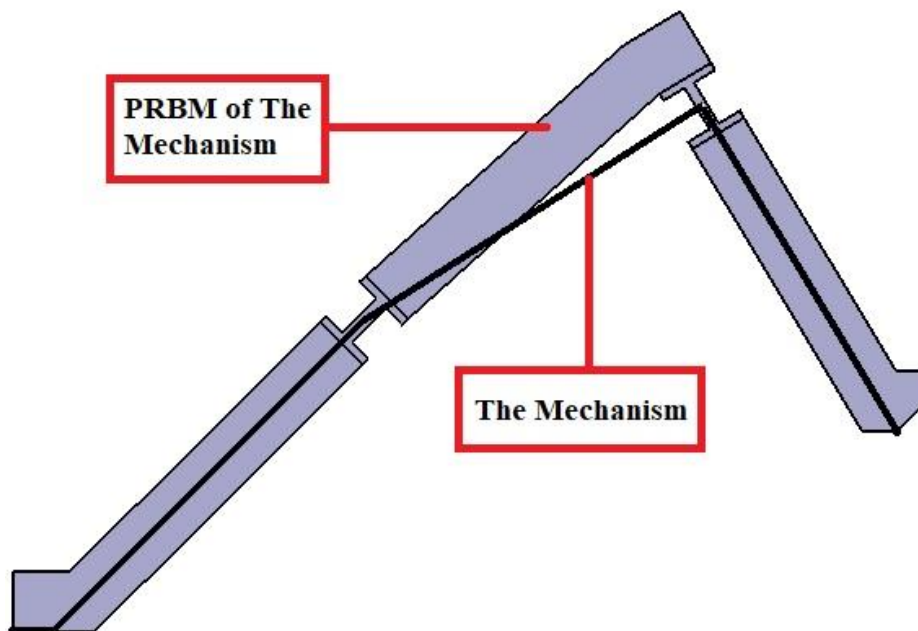


Figure 29: PRBM of the mechanism.

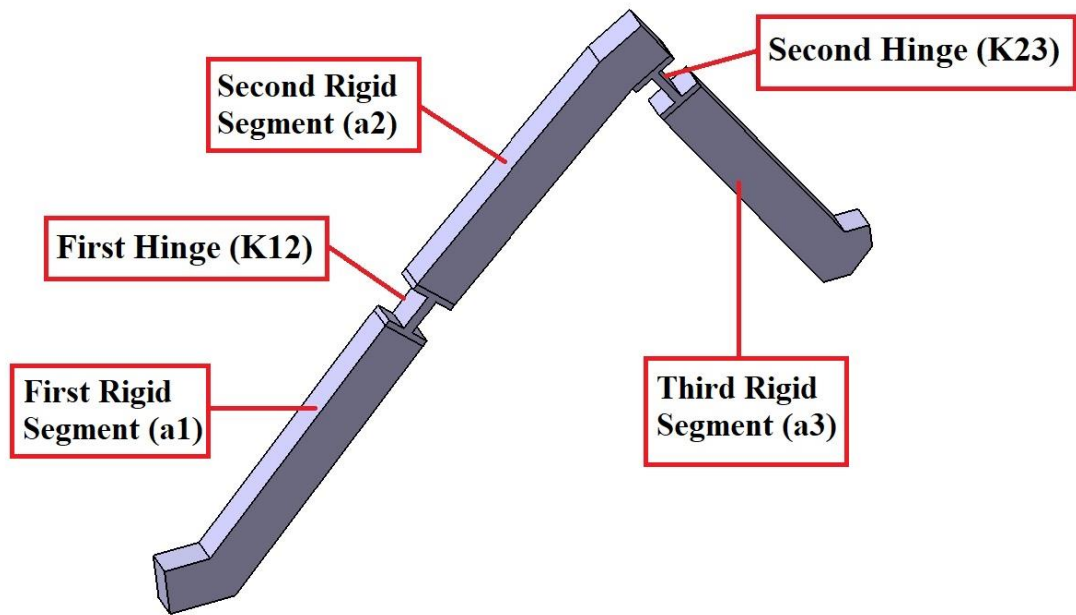


Figure 30: Geometry model of the mechanism.

The mechanism whose dimensions are given above is modeled as three separate links and two separate hinges (Figure 30). The purpose of drawing in this way is to be able to apply mesh in different sizes. In addition, 2 mm length from both ends of both hinges is left for a more accurate distribution of tension (Figure 31).

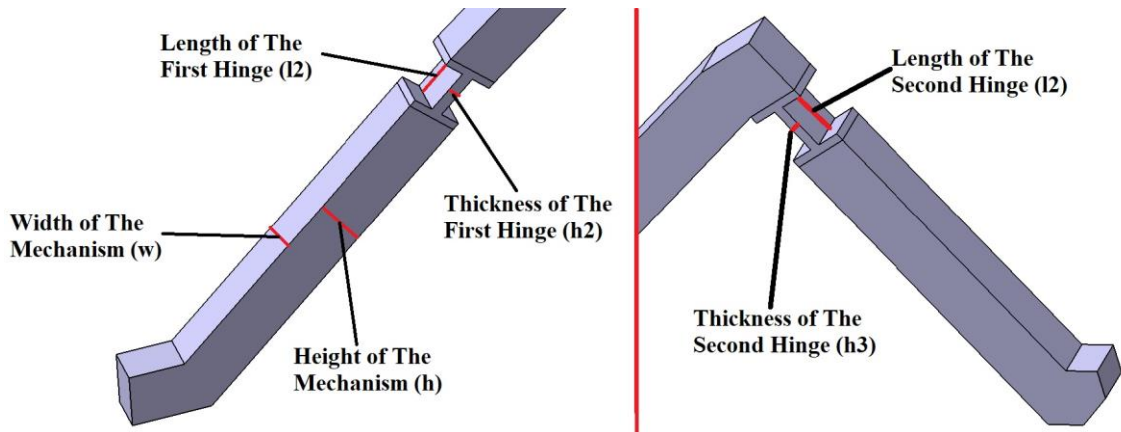


Figure 31: Detail of the mechanism.

The created model is converted to STP file format and transferred to the geometry tab of the Ansys Static Structural module (Figure 32), and the model of the mechanism is prepared for verification.

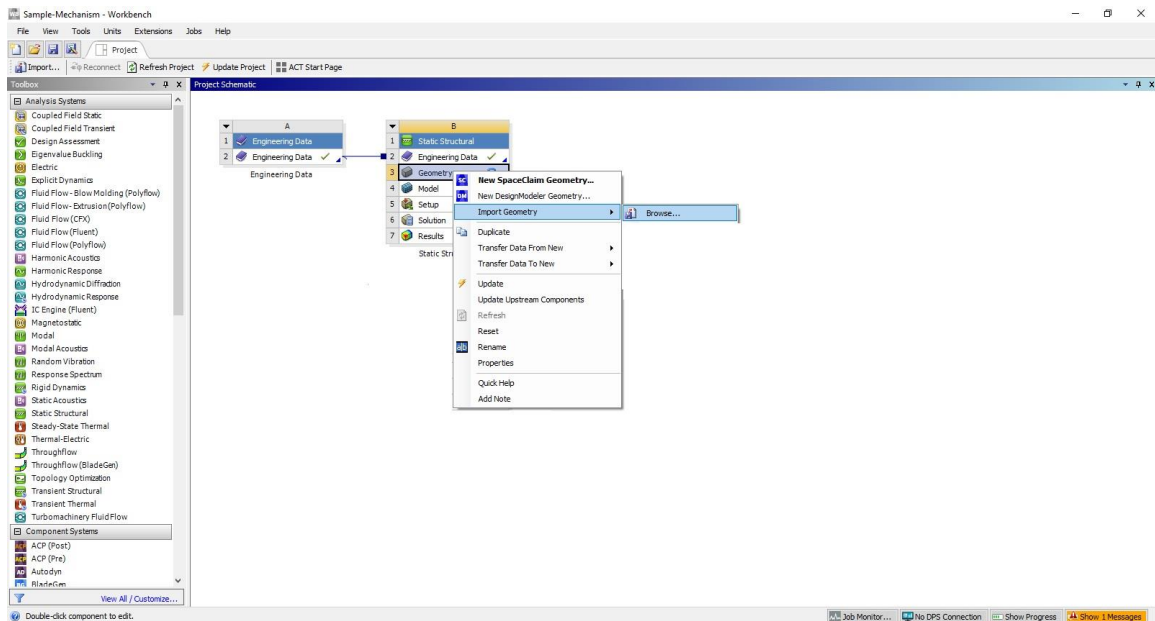


Figure 32: Importing the 3D model.

4.3. Generating Model of the Mechanism

After selecting the material and transferring the 3D model, the mechanism is modeled. For this, the Model tab of Ansys Structural opens. The previously created Polypropylene material is assigned to the model (Figure 33). After the material assignment is made, the Mesh is applied. In order for the mechanism analysis to give accurate results and the solution time not to be long, a mesh with different element sizes is created on the hinges from the links of the mechanism. Also, first, second and third link is chosen as a rigid body. The element size of the mesh created for the hinges is 0.75 mm (Figure 34). In addition, the mesh consists of 4 layers on the thickness of the hinges (Figure 35). Thus, a smooth mesh web consisting of 28441 cells and 5827 elements is applied for the mechanism analysis.

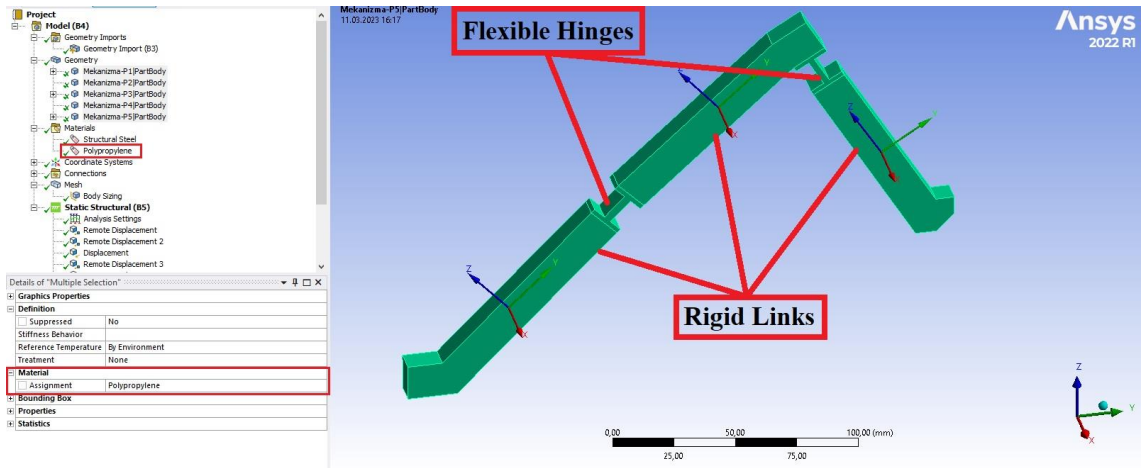


Figure 33: Material selection.

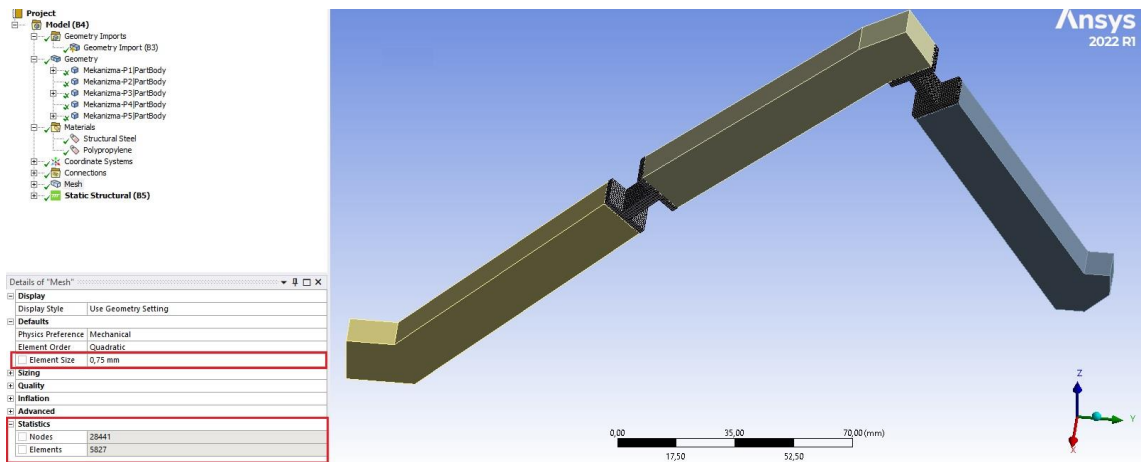


Figure 34: Meshing of the mechanism.

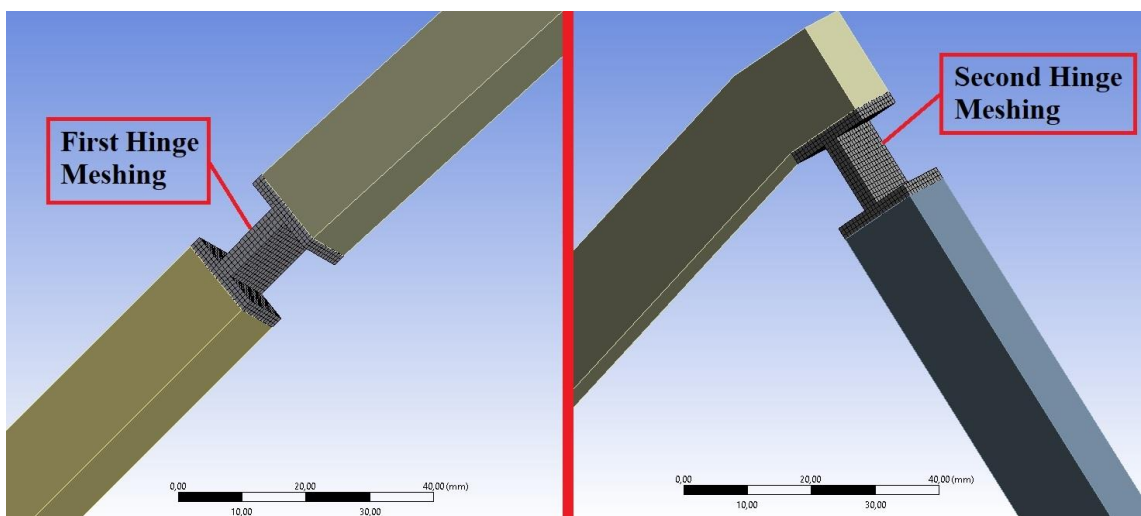


Figure 35: Mesh detail.

Analysis adjustments are made after the meshing process is completed. At this stage, in order to see the displacement step by step and to interpret the analysis, the "Auto Time Stepping" tab under "Step Controls" heading is activated. Later, the "Define By" tab is selected as "Time". Then, the "Initial Time Step", "Minimum Time Step" and "Maximum Time Step" tabs are designated as "0.01", "0.001" and "0.01", respectively. Also, the entire analysis is set to finish in one second. In addition, since the deformation of the hinges exhibits a non-linear behavior, analysis is performed by turning on "Weak Springs" and "Large Deflection Mode" (Figure 36).

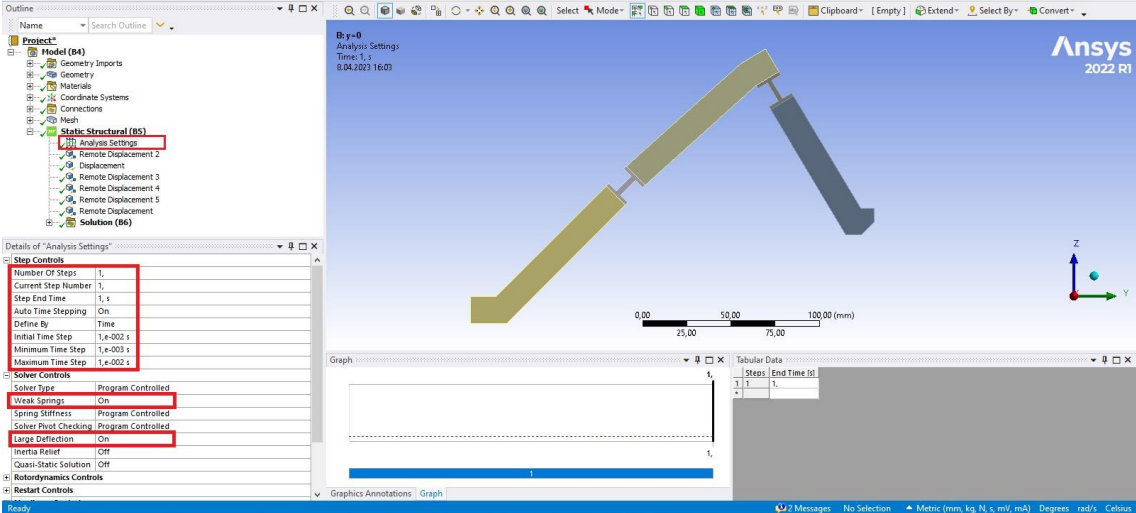


Figure 36: Analysis settings.

After the analysis adjustments are completed, a fixed support surface is selected for the analysis of the mechanism. This support surface should be chosen to simulate real conditions. Therefore, the starting surface of the fixed member of the mechanism is designated as the fixed support. But, as first, second and third links are chosen as rigid body, remote displacement must be applied to the starting surface to all of the six components being zero (Figure 37). Additionally, a displacement on a side of hinges and remote displacements on a side of links are applied to obstruct moving at X axis (Z axis in mathematical model). Also, the "Contact Region" connections automatically assigned by Ansys are rearranged between the hinges and segments of the mechanism. Because the links are chosen as rigid segments, the contact surfaces are first chosen as hinges and then rigid segments (Figure 38). Then, a remote displacement is assigned in the Z axis (Y axis in mathematical model) direction to simulate the displacement of the mechanism. In addition, since the movement of the mechanism in the Y axis (X axis in mathematical model) is assumed to be constant in the mathematical model, the Y component of this

remote displacement is entered as "0 mm". So, in this way, the validity of the acceptance is analyzed. Thus, during the calculations it is comprehended that the mechanism increased from 50 mm to 130 mm along the Z axis (Y axis in mathematical model), and is constant in the Y axis (X axis in mathematical model). In addition, the selection of the displacement point is chosen to overlap on the 3D model with the PRBM adaptation (Figure 39), as in Figure 18, where the calculations are made (Figure 40). Because, this is a very important factor in correctly reading the reaction force and making comparisons with numerical calculations. As a result, in order to determine the accuracy of the analytical solution, it is essential that the analysis to be done is suitable for the real application and that the boundary conditions are the same.

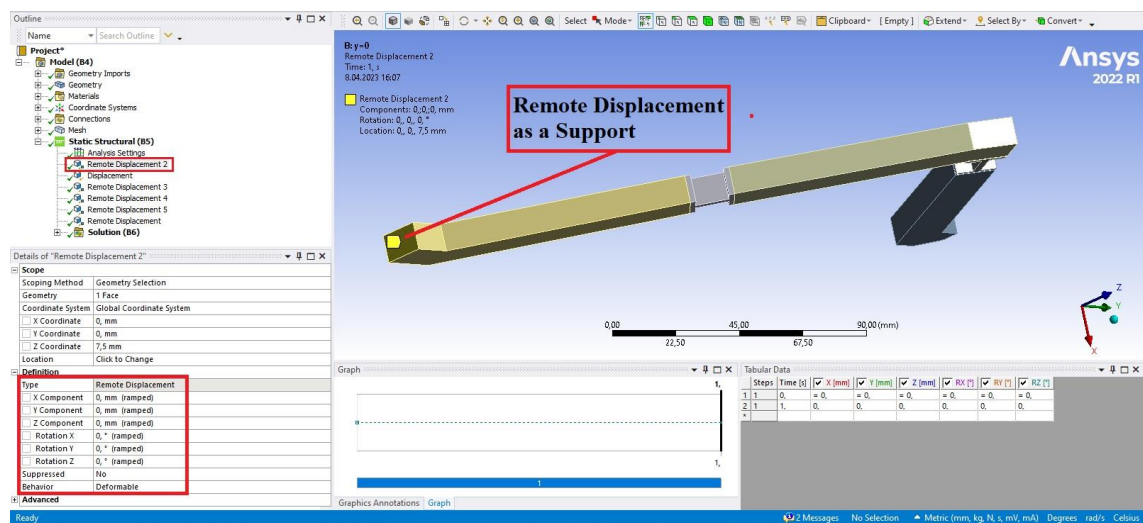


Figure 37: Fixed support of the mechanism.

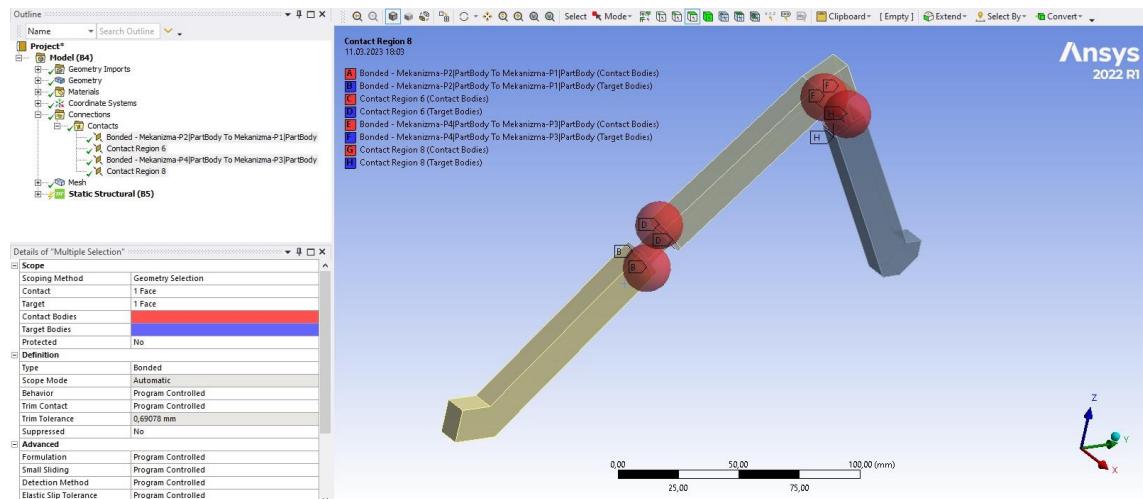


Figure 38: Contacts of the links and hinges.

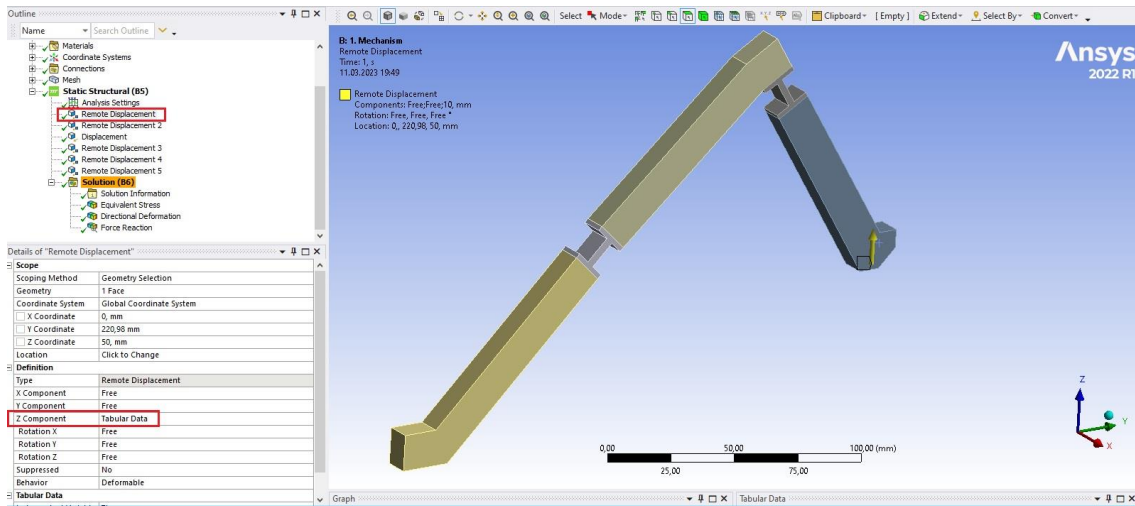


Figure 39: Applying remote displacement.

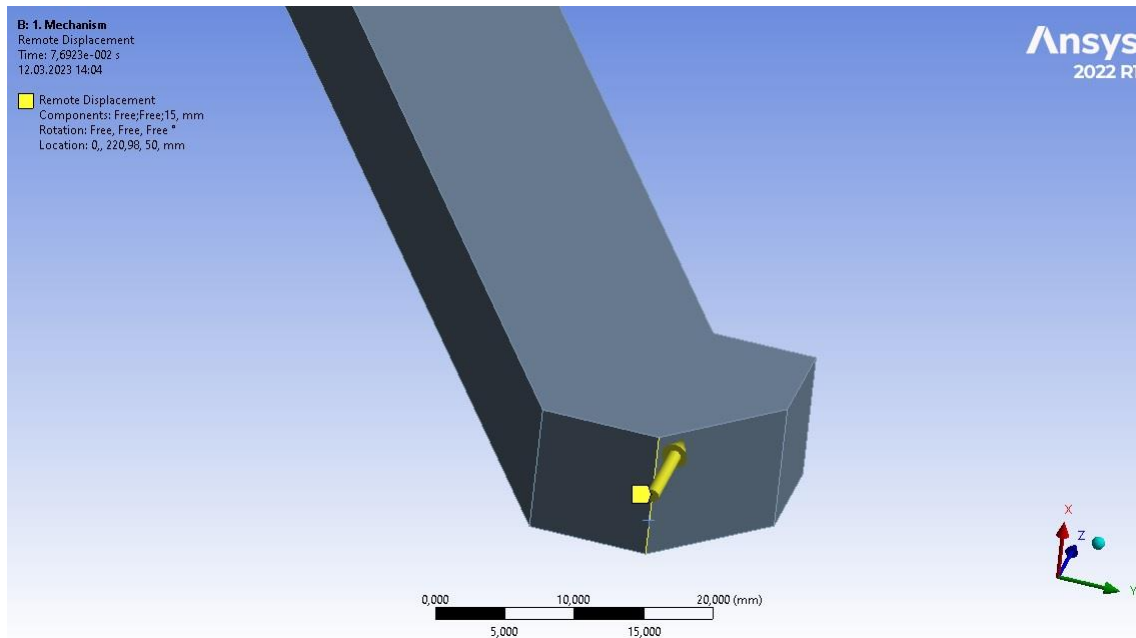


Figure 40: Selection of the displacement point.

4.4. Solutions of the Mechanism

After making the analysis settings of the optimized mechanism, analysis is performed to control the reaction force and equivalent stress (Von-Mises) values (Figure 41). So, in order to understand whether the analysis is converged or not, the force converge graph is examined in the solution information (Figure 42). Then, the reaction force obtained from the analysis is compared with the reaction force obtained from the numerical analysis, and it is interpreted whether a constant force is obtained or not (Figure 43).

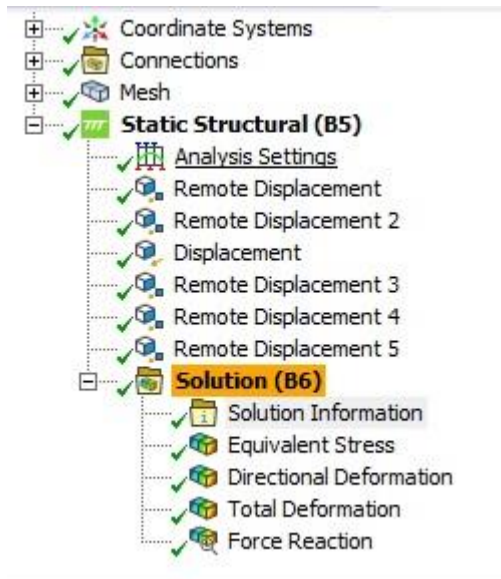


Figure 41: Solutions of the mechanism.

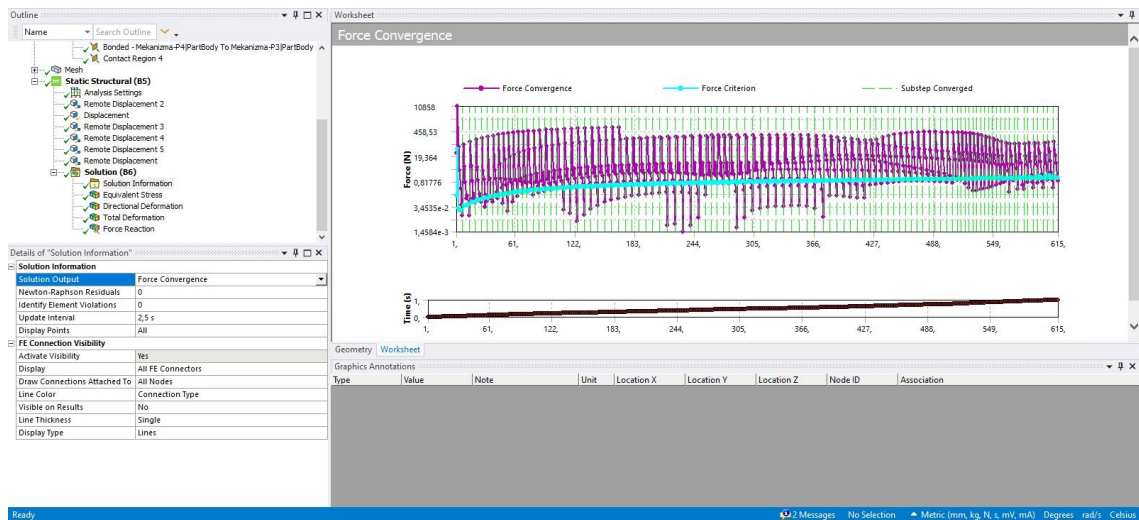


Figure 42: Force converge diagram of the mechanism.

As can be seen from the force converge diagram above, the analysis is solved non-linearly in 615 iterations and converged.

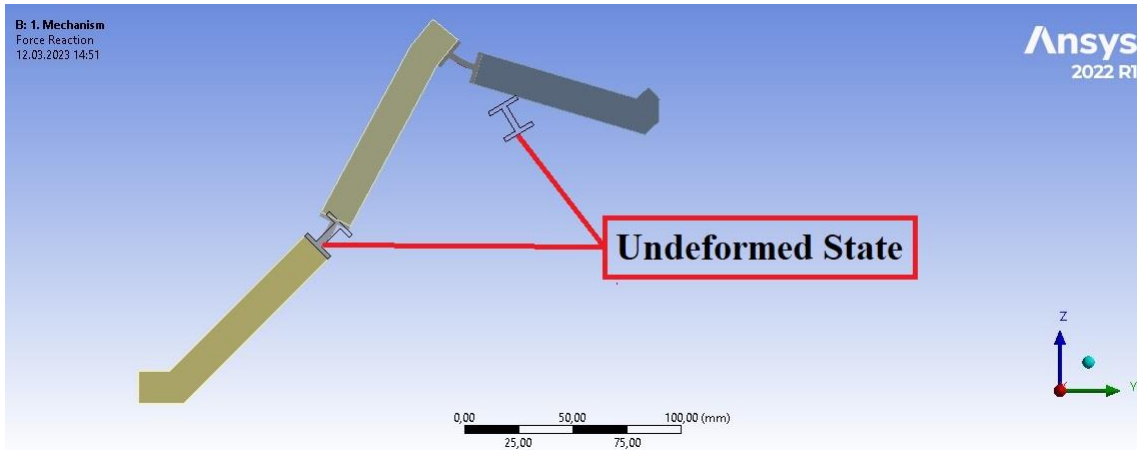


Figure 43: Force reaction solution of the mechanism.

Figure 44 shows comparisons of Matlab and Ansys reaction force. The curve in blue refers to data from Matlab, the curve in orange refers to data from Ansys. In addition, the horizontal axis of the graph shows the displacement of the mechanism (Matlab -Y axis, Ansys -Z axis), while the vertical axis shows the reaction forces obtained. In this context, when the change graph of Matlab data is examined, the average rate of change is 5.61%. This rate of change is sufficient for the compliant mechanism and is expected to remain below 10% [15]. Likewise, when Ansys data is examined, the average rate of change is 8.62%, below 10%. Moreover, the difference between them with numerical analysis is 7.23%. As a result, as can be understood from the ratio between the mathematical model and the analysis, a Constant Force Compliant Mechanism is designed in accordance with the purpose of this thesis.

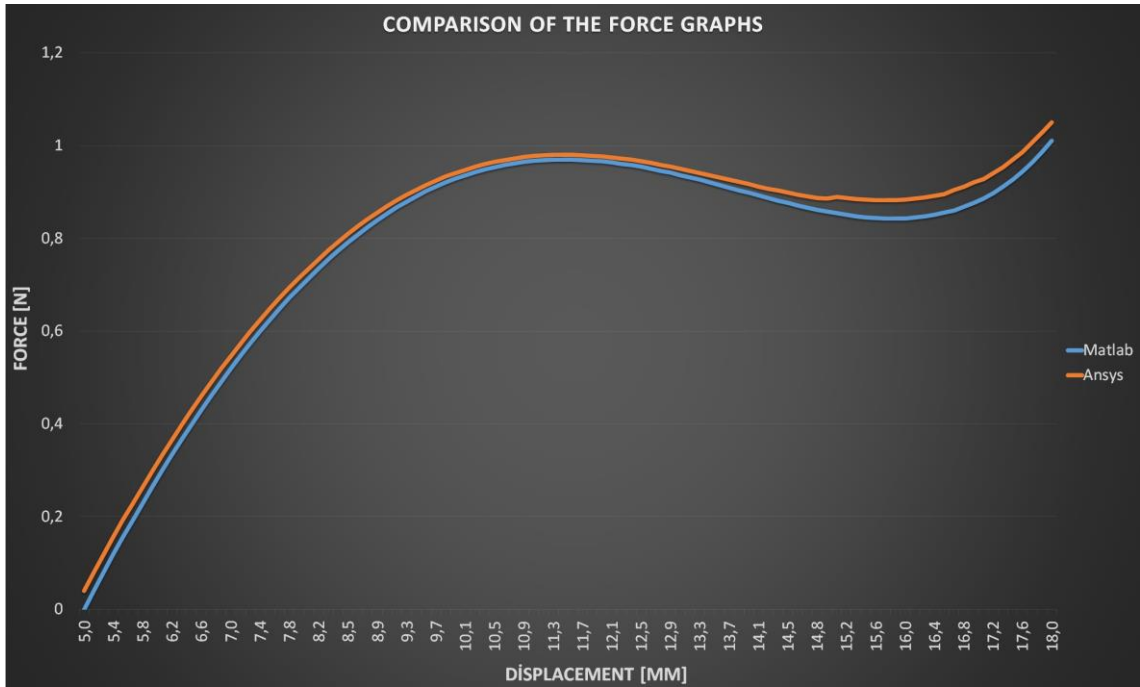


Figure 44: Comparison of the mechanism.

Finally, the equivalent stress (von-Mises) distribution of the mechanism is examined in Figures 45 and 46. The tensile yield strength of the material given in Table 2 is 35 MPa. As a result of the analysis, the maximum stress on the mechanism is 33.752 MPa. When the resulting stresses are evaluated, it is comprehended that the stresses are at the limit values. Therefore, the maximum y-axis movement of the mechanism is approached. However, for the purpose of the study, the stress distribution for this displacement is acceptable.

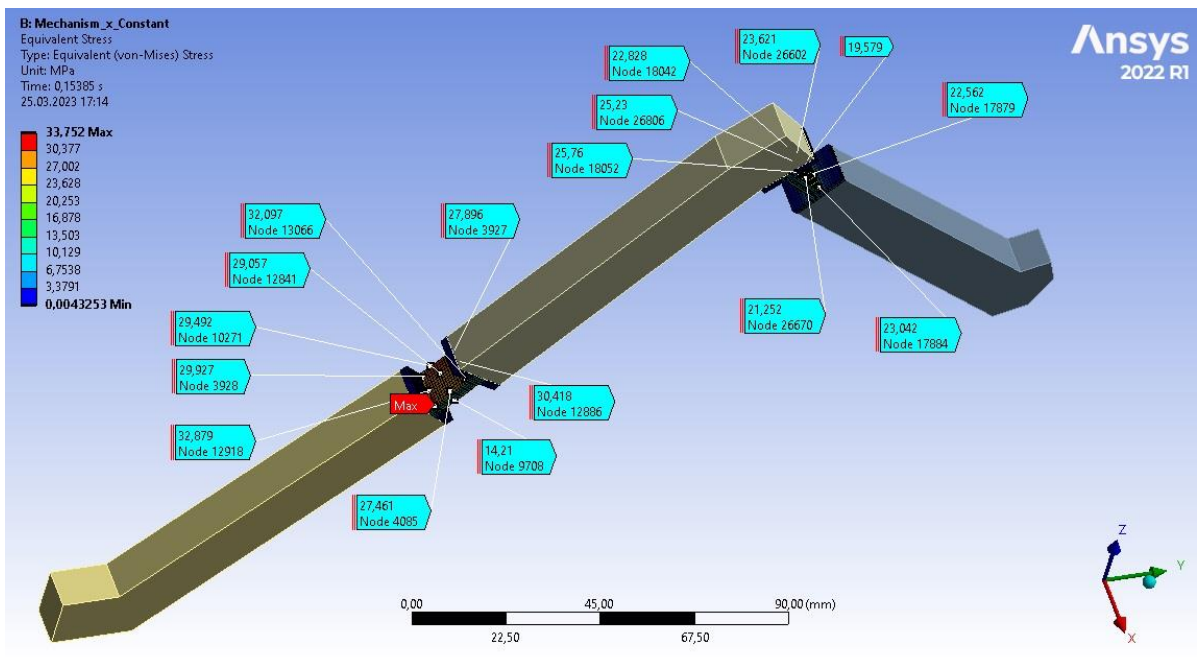
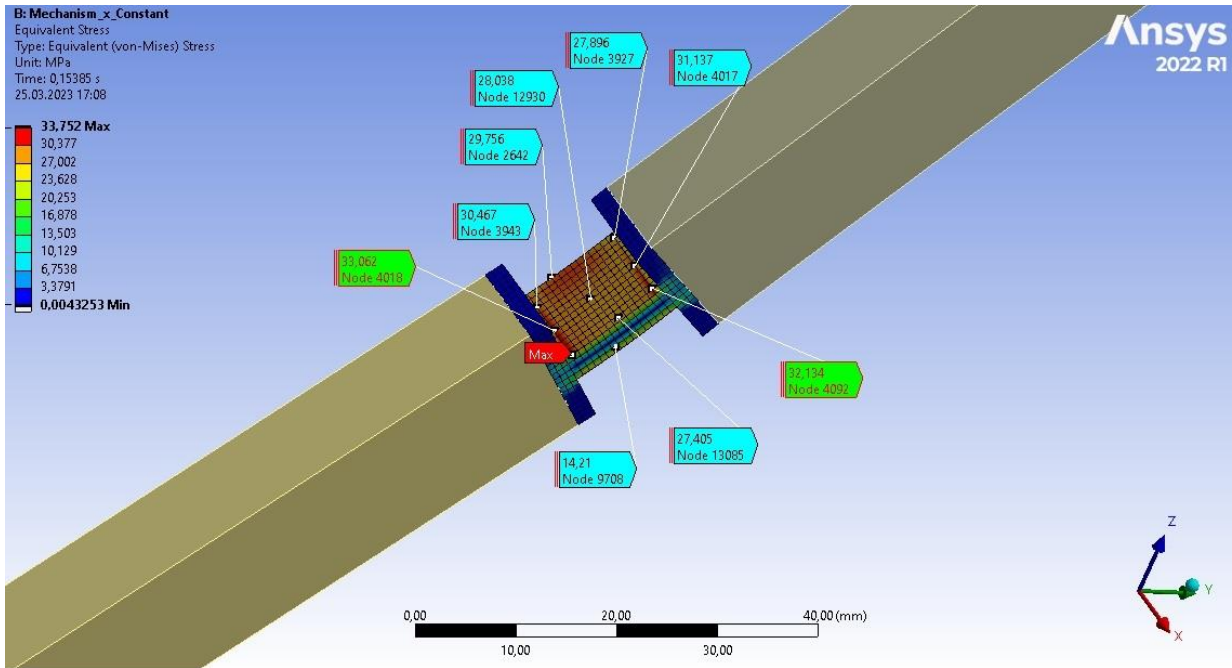
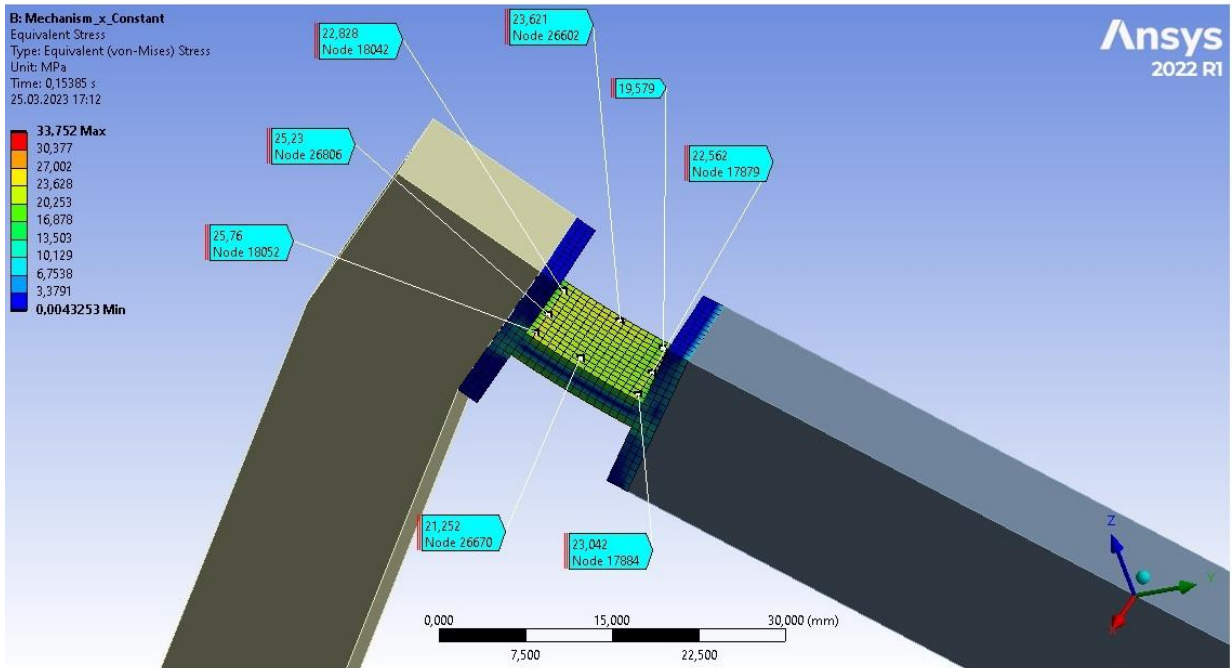


Figure 45: Equivalent stress of the mechanism.



a)



b)

Figure 46: Detailed equivalent stress a) First Hinge b) Second Hinge
 The mathematical model of the mechanism is verified by the analysis study.

5. CONCLUSION

Constant-Force Compliant Mechanism has been gaining serious importance recently and researches are being done in this field. One of the biggest reasons for gaining importance is that traditional mechanisms need a large number of sensors and a complex structure in order to generate constant force. Therefore, constant-force mechanisms created by traditional methods are produced quite expensive and complex. Thus, constant-force compliant mechanisms constitute an important alternative due to their low cost and simple structure.

Although the mechanism that produces constant force in theory is mentioned, in reality, a certain fluctuation is to occur when the force is first produced, then the fluctuations is to be damped and continue at a constant proportion. As it can be understood from here, a transition zone is needed to reach the desired force. That is, the purpose of the constant force mechanism is to minimize the fluctuations in this transition region.

In this study, a novel constant-force compliant gripper mechanism with two degrees of freedom, one side fixed and the other side free, is proposed. Therefore, the aim of this study is to construct a CFCM that minimizes force fluctuations when the mechanism is displaced from its free end and in which all its links are optimized. However, in this study, a solution is sought by accepting the x value as constant due to time constraints. In future studies, optimization of the mechanism links will be made by limiting the solution range of the θ_2 angle and making it continuous. Then, it is to be examined whether the optimized mechanisms produce constant force. Subsequently, the production of the mechanism is to be fulfilled and the numerical and analysis data will be compared and this subject is to be published with a paper.

First of all, closed-loop equations of the mechanism are created with PRBM, which is an efficient method for CFCM. Subsequently, other necessary equations are extracted from by using the virtual work method. Then, by combining these equations, the necessary equations were derived to find the unknowns of the mechanism. Afterward, all these equations are made unitless for ease of calculation. After creating all the necessary equations, a basic code is written to solve the equations. This code is created with the Multivariable Newton-Raphson Method. However, at this point, this movement is neglected as it is known that the movement of the mechanism in the X axis is to be quite low. Therefore, the mechanism is assumed to be constant in the X axis. In line with

this acceptance, all the equations of the mathematical model are rearranged and a different code is written. Subsequently, the range of constant force is found by optimizing the mechanism members. The solid model of the mechanism, the design of which is completed, is prepared and the analysis phase is passed. At this stage, the reaction force of the optimized constant force generating mechanism is investigated by applying displacement in accordance with the mathematical model. The mechanism design is completed by comparing these reaction force data with the constant force data obtained from the mathematical model.

As a result, it is observed that approximate constant force mechanisms can be designed by the proposed method. A design example is displayed and it is shown that an approximate constant force can be obtained for a large stroke. Thus, different sized objects can be held with the same force with this gripper. The mechanism is analyzed by FEA and analytical results are verified. Also, it is observed that the maximum stresses are in acceptable region.

REFERENCES

- [1] LARRY L, H., Compliant mechanisms. A Wiley-Interscience Publication, New York, **2001**.
- [2] Senapati, S., “Compliant mechanisms”, Retrieved from IEEE: <https://iee.nitk.ac.in/blog/compliant-mechanisms/>, (Access date: **08 July 2017**).
- [3] Tanık, Engin, “Transmission angle in compliant slider-crank mechanism” Vol.46 (11), 1623-1632, Mechanism and Machine Theory, Elsevier, **2011**.
- [4] Rushikesh S. Joshi, A. C., “Design and analysis of compliant micro-gripper using pseudo rigid body model”, Vol.4 (2), 1701-1707, Materials Today, **2017**.
- [5] Parlaktaş, V., “Spatial compliant constant-force mechanism”, Vol. 67, 152-165, Mechanism and Machine Theory, Elsevier, **2013**.
- [6] Duc-Chuong Nguyen, T.-V. P.-T., Design and analysis of a compliant gripper Integrated with constant-force and static balanced mechanism for micro manipulation, 4th Int. Conf. on Green Tech. and Sust. Dev. Ho Chi Minh City, 23-24 November 2018, Vietnam: IEEE., Ho Chi Minh City, **2018**.
- [7] Weihai Chen, J. Q., “A compliant dual-axis gripper with integrated position and force sensing”, Vol. 47, 105-115, Mechatronics, Elsevier, **2017**.
- [8] Tanık, Engin, Söylemez, Eres, “Analysis and design of a compliant variable stroke”, Vol. 45 (10) 1385-1394, Mechanism and Machine Theory, Elsevier, **2010**.
- [9] Piyu Wang, Q. X., “Design and modeling of constant-force mechanism”, Vol. 119, 1-21, Mechanism and Machine Theory, Elsevier, **2007**.
- [10] Tanık, Engin, “Fully compliant spatial four-bar mechanism”, vol. 9, (1), AMDSM0002- JAMDSM0002, Journal of Advanced Mechanical Design, System and Manufacturing, **2015**.
- [11] Parlaktaş, Volkan, Tanık, Engin, & Tanık, Çağıl Merve, “On the design of a novel fully compliant spherical four-bar mechanism”, Vol. 11 (9), 1-12, SAGE Journals, **2019**.
- [12] Tanık, Çağıl Merve, On the analysis and design of a novel fully compliant slider-crank mechanism, Master Degree Thesis, Middle East Technical University Graduate School of Natural and Applied Sciences, Ankara, **2020**.

- [13] Kyler A. Tolman, E. G., “Compliant constant-force linear-motion mechanism”, Vol. 106, 68-79, Mechanism and Machine Theory, Elsevier, **2016**.
- [14] Dalibor Petkovic, M. I., “Adaptive neuro fuzzy controller for adaptive compliant robotic gripper”, Vol. 39 (18), 13295-13304, Expert Systems with Applications, Elsevier, **2012**.
- [15] Kayalı, Oğuz, Design of a constant force compliant gripper mechanism, Hacettepe University Graduate School of Science and Engineering, Ankara, **2019**.
- [16] Muhammed Gaafar, M. M.-B., Development of a new compliant remote center of motion mechanism for vitreoretinal surgery, 6th. Int. Conf. on Cntrl., Automation. And robotics. Singapore, 20-23 April 2020, IEEE, Singapore, **2020**.
- [17] Rahman, M. U., “Design of constant force compliant mechanisms”, International Journal of Engineering Research and Technology, Vol. 3 (7), 758-769, **2014**.
- [18] Işıkdoğan, İsa Ömer, Design and analysis of a novel compliant constant force gripper. Hacettepe University Graduate School of Science and Engineering, Ankara, **2020**.

APPENDIX

Appendix 1 – The Design Codes

```
clc; clear all; close all; format longg;

%% Parameters adaptation
% Theta2=z, Theta3=v

%% Values
% Length and angle of the links
C=45*pi/180; % Angle of the first link (Constant) [Rad]
a1=11; % Length of the constant link [mm]
a2=10; % Length of the second link [mm]
C2=32.480784405447324*pi/180; % Initial value of the Theta 2 [Rad]
a3=9.5; % Length of the third link [mm]
% Constant spring force of the mechanism
k12=40; % First spring force constant
k13=20; % Second spring force constant
% Input
j=0:13;
o=5;
Y=j+o; % Stroke of the mechanism at the Y-Axis [mm]
% Assumption
% Stroke of the mechanism at the X-Axis is constant
% Index
i=1;

%% Optimized mechanism calculation
for i=1:14 % Calculation for every value of the input Y
    C3_Cd=asin((a1*sin(C)+a2*sin(C2)-Y(1))/a3)*180/pi; % Complementary
    angle of the Theta 3 [Deg]
    C3_d=360-C3_Cd; % Angle of the Theta 3 [Deg]
    C3=C3_d*pi/180; % Angle of the Theta 3 [Rad]
    xiii=a1*cos(C)+a2*cos(C2)+a3*cos(C3); % Initial value of the
    mechanism at the X-Axis for verification [mm]
    yiii=a1*sin(C)+a2*sin(C2)+a3*sin(C3); % Initial value of the
    mechanism at the Y-Axis for verification [mm]
    x=a1*cos(C)+a2*cos(C2)+a3*cos(C3); % Initial value of the
    mechanism at the X-Axis [Constant] [mm]
    l(i)=(((x-a1*cos(C))^2+(Y(i)-a1*cos(C))^2)^(1/2));
    Alfa(i)=acos((a2^2-a3^2+l(i)^2)/(2*a2*l(i)));
    Alfad(i)=Alfa(i)*180/pi;
    Gamma(i)=atan((Y(i)-a1*sin(C))/(x-a1*sin(C)));
    Gammad(i)=Gamma(i)*180/pi;
    z(i)=(Alfa(i)+Gamma(i));

    A(i)=acos((x^2+Y(i)^2+a1^2-a2^2-a3^2-
2*a1*(x*cos(C)+Y(i)*sin(C)))/(2*a2*a3));
    v(i)=2*pi+z(i)-A(i);

    div32(i)=((-a2*sin(z(i)))/(a3*sin(v(i))));
    Aa(i)=k12*(z(i)-C2);
    Bb(i)=k13*(v(i)-z(i)+C2-C3)*(div32(i)-1);
    Cc(i)=(a2*cos(z(i)));
    Dd(i)=(a3*cos(v(i))*div32(i));
    Ff(i)=(Aa(i)+Bb(i))/(Cc(i)+Dd(i));
```

```

    F(i)=(k12*(z(i)-C2)+k13*(v(i)-z(i)+C2-C3)*(div32(i)-
1))/((a2*cos(z(i))+a3*cos(v(i))*div32(i)));
    Theta2(i)=z(i)*180/pi;
    Theta3(i)=v(i)*180/pi;
end

%% Length Calculation of Hinges
% First hinge
E= 1500; % Elasticity module [N/mm^2]
w=10; % width of the flexible joint [mm]
l_2=1.2;
I_2=(l_2*k12)/E;
h_2=(I_2*12/w)^(1/3);
%h_2=1; % height of the second flexible joint [mm]
%I_2=(w*(h_2)^3)/12; %inertia of the second flexible joint
%l_2=(E*I_2)/k12;
% Second hinge
K=k12/k13;
l_3=1.2;
h_3=((h_2^3)*l_3)/(K*l_2)^(1/3); %height of the third flexible joint
I_3=(w*(h_3)^3)/12; %inertia of the second flexible joint

%% 2D Plot
i = 1:10;
figure (1);
plot(Y, Theta2)
set (gca, 'FontSize', 10)
xlabel ('Y [mm] (Displacement at the -y axis)', 'FontSize', 12)
ylabel ('Theta 2 [°]', 'FontSize', 12)
title('The Angle of The Theta 2', 'FontSize', 12)
grid on;

i = 1:10;
figure (2);
plot(Y, Theta3)
set (gca, 'FontSize', 10)
xlabel ('Y [mm] (Displacement at the -y axis)', 'FontSize', 12)
ylabel ('Theta 3 [°]', 'FontSize', 12)
title('The Angle of The Theta 3', 'FontSize', 12)
grid on;

i = 1:10;
figure (3);
plot(Y, F)
set (gca, 'FontSize', 10)
xlabel ('Y [mm] (Displacement at the -y axis)', 'FontSize', 12)
ylabel ('Force [Nm]', 'FontSize', 12)
title('The Constant Force Values of The Mechanism', 'FontSize', 12)
grid on;

```